Co-occurrence of rhizobacteria with nitrogen fixation and/or 1-aminocyclopropane-1-carboxylate deamination abilities in the maize rhizosphere

Sébastien Renoud, Marie-Lara Bouffaud, Audrey Dubost, Claire Prigent-Combaret, Laurent Legendre, Yvan Moenne-Loccoz, Daniel Muller

OXFORD UNIVERSITY PRESS | FEMS Microbiology Ecology

http://mc.manuscriptcentral.com/fems

Co-occurrence of rhizobacteria with nitrogen fixation and/or 1-aminocyclopropane-1-carboxylate deamination abilities in the maize rhizosphere

Journal:	*FEMS Microbiology Ecology*
Manuscript ID	FEMSEC-20-01-0023.R2
Manuscript Type:	Research article
Date Submitted by the Author:	n/a
Complete List of Authors:	Renoud, Sébastien; Université de Lyon, Université Claude Bernard Lyon 1 UMR5557 Bouffaud, Marie-Lara; Université de Lyon, UMR CNRS 5557 Ecologie Microbienne Dubost, Audrey; Universite Claude Bernard Lyon 1 Faculte des Sciences et Technologies, UMR 5557 Microbial Ecology Laboratory Prigent-Combaret, Claire; Université de Lyon, UMR CNRS 5557 Ecologie Microbienne Legendre, Laurent; Université de Lyon, UMR5557 Moënne-Loccoz, Yvan; Université de Lyon, UMR CNRS 5557 Ecologie Microbienne Muller, Daniel; Université de Lyon, UMR5557
Keywords:	microbiota, plant growth promotion, functional group, functional microbiota, holobiont, ITSNTS theory

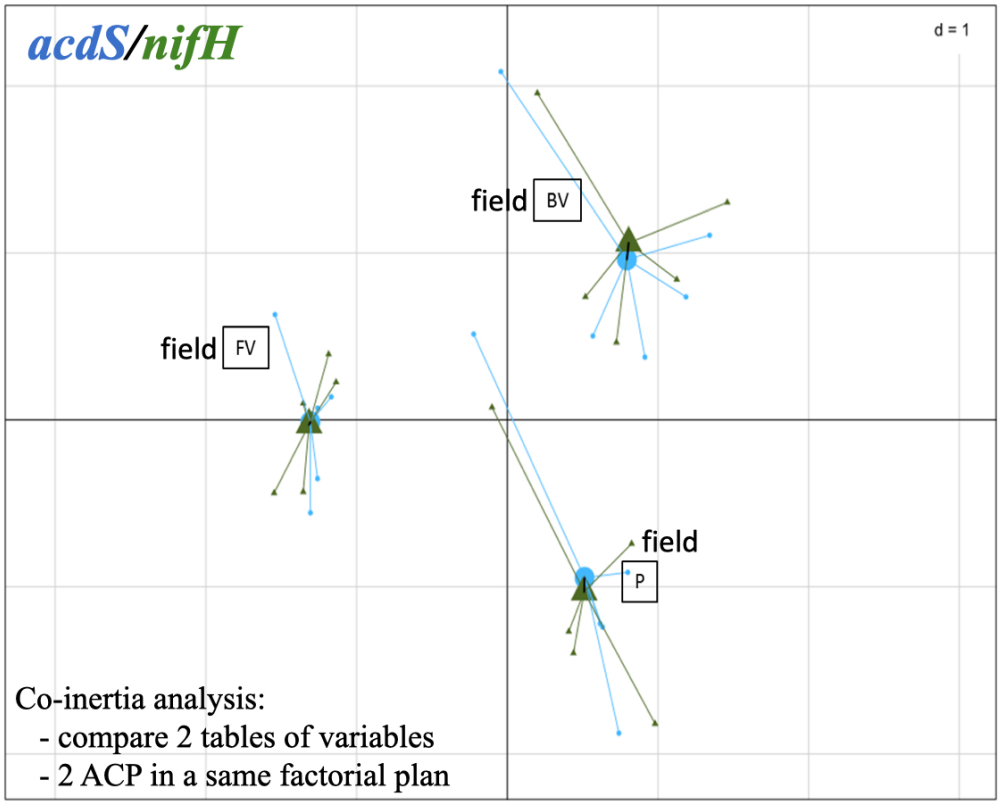

395x318mm (72 x 72 DPI)

Co-occurrence of rhizobacteria with nitrogen fixation and/or 1-aminocyclopropane-1-carboxylate deamination abilities in the maize rhizosphere

Sébastien Renoud[1‡], Marie-Lara Bouffaud[1‡], Audrey Dubost[1], Claire Prigent-Combaret[1], Laurent Legendre[1,2], Yvan Moënne-Loccoz[1] and Daniel Muller[1*]

[1] Univ Lyon, Université Claude Bernard Lyon 1, CNRS, INRAE, VetAgro Sup, UMR5557 Ecologie Microbienne, 43 bd du 11 novembre 1918, F-69622 Villeurbanne, France

[2] Univ Lyon, Université de St Etienne, F-42000 St Etienne, France

‡ Current addresses:

S.R. : BGene genetics Bâtiment B Biologie, F-38400 Saint Martin d'Hères, France

M.L.B. : Helmholtz Center for Environmental Research UFZ, Theodor-Lieser-Straβe 4, 06120 Halle, Germany

Running title: *nifH* and *acdS* bacteria on maize

***Corresponding author:** UMR CNRS 5557 Ecologie Microbienne, Université Lyon 1, 43 bd du 11 Novembre 1918, 69622 Villeurbanne cedex, France. Phone: +33 4 72 43 27 14. E-mail: daniel.muller@univ-lyon1.fr

ABSTRACT

The plant microbiota may differ depending on soil type, but these microbiota probably share the same functions necessary for holobiont fitness. Thus, we tested the hypothesis that phytostimulatory microbial functional groups are likely to co-occur in the rhizosphere, using groups corresponding to nitrogen fixation (*nifH*) and 1-aminocyclopropane-1-carboxylate deamination (*acdS*), i.e. two key modes of action in plant-beneficial rhizobacteria. The analysis of three maize fields in two consecutive years showed that quantitative PCR numbers of *nifH* and of *acdS* alleles differed according to field site, but a positive correlation was found overall when comparing *nifH* and *acdS* numbers. Metabarcoding analyses in the second year indicated that the diversity level of *acdS* but not *nifH* rhizobacteria in the rhizosphere differed across fields. Furthermore, between-class analysis showed that the three sites differed from one another based on *nifH* or *acdS* sequence data (or *rrs* data), and the bacterial genera contributing most to field differentiation were not the same for the three bacterial groups. However, co-inertia analysis indicated that the genetic structures of both functional groups and of the whole bacterial community were similar across the three fields. Therefore, results point to co-selection of rhizobacteria harboring nitrogen fixation and/or 1-aminocyclopropane-1-carboxylate deamination abilities.

Keywords: microbiota; phytostimulation; functional group; functional microbiota; holobiont; ITSNTS theory

INTRODUCTION

Plant Growth-Promoting Rhizobacteria (PGPR) colonize plant roots and implement a range of plant-beneficial traits, which may result in enhanced plant development, nutrition, health and/or stress tolerance (Almario et al. 2014; Cormier et al. 2016; Gamalero and Glick 2015; Hartman et al. 2018; Vacheron et al. 2013). As a consequence, PGPR strains have received extensive attention for use as microbial inoculants of crops (Bashan et al. 2014; Couillerot et al. 2013).

Plant-beneficial effects exhibited by PGPR are underpinned by a wide range of modes of actions, which include (i) enhanced nutrient availability via associative nitrogen fixation (Puri et al. 2016, Deynze et al. 2018) or phosphate solubilization (Arruda et al. 2013), (ii) stimulation of root system establishment through phytohormone synthesis (Cassán et al. 2014) or consumption of the ethylene precursor 1-aminocyclopropane-1-carboxylate (ACC) via an enzymatic deamination (Glick 2014), and (iii) the induction of systemic resistance responses in plant (Pieterse and Van Wees 2015). In addition to phytostimulation, certain PGPR may also achieve inhibition of phytoparasites using antimicrobial secondary metabolites (Agaras et al. 2015) or lytic enzymes (Pieterse and Van Wees 2015). Often, PGPR strains display more than one phytostimulatory mode of action, which is considered important for effective plant-beneficial effects (Bashan and de-Bashan 2010; Bruto et al. 2014; Rana et al. 2011; Vacheron et al. 2017). Therefore, the co-occurrence of multiple phytostimulation traits is likely to have been subjected to positive evolutionary selection in PGPR populations to maximize success of the plant-PGPR cooperation. This hypothesis is substantiated by genome sequence analysis of many prominent PGPR strains from contrasted taxa (Bertalan et al. 2009; Chen et al. 2007; Redondo-Nieto et al. 2013; Wisniewski-Dyé et al. 2012).

Even though PGPR strains tend to accumulate several plant-beneficial traits (Bruto et al. 2014), the co-occurrence patterns of these traits are not random. This takes place in part

because many past horizontal gene transfers of the corresponding genes were ancient (Frapolli et al. 2012), often leading to clade-specific profiles of plant-beneficial traits (Bruto et al. 2014). However, the analysis of 304 proteobacterial genomes from contrasted taxa evidenced, overall, the co-occurrence of *nifHDK* (nitrogen fixation) and *acdS* (ACC deamination) based on Exact-Fisher pairwise tests (Bruto et al. 2014), raising the possibility that nitrogen fixation and ACC deamination might be useful traits when combined in a bacterium. Indeed, nitrogen fixation and ACC deamination occur together in various rhizobacteria (Blaha et al. 2006; Duan et al. 2009; Jha et al. 2012; Ma, Guinel, and Glick, 2003; Nukui et al. 2006), but the relation between both traits can be complex. In *Azospirillum lipoferum* 4B for instance, the plasmid-borne gene *acdS* is eliminated during phase variation while *nif* genes are maintained (Prigent-Combaret et al. 2008), and in *Mesorhizobium loti* transcription of *acdS* is controlled by the nitrogen fixation regulator gene *nifA2* (Nukui et al. 2006). Moreover, ACC deamination was described as facilitator of the legume-rhizobia symbiosis (Ma et al. 2003; Nascimento et al. 2012).

At the scale of an individual plant, the rhizosphere is colonized by a diversified range of bacteria, including *nifH acdS* bacteria as well as bacteria harboring only *nifH* or *acdS* (Blaha et al. 2006; Bouffaud et al. 2018). There is additional level of complexity in that many of these bacteria are PGPR, but some of them are not (Bruto et al. 2014). However, the overall impact of nitrogen fixation and ACC deamination on the plant is likely to be the sum of the contribution of individual root-colonizing bacteria displaying these traits. This raises the question whether there is, for the plant, an optimal balance between the functional microbial groups of *nifH* rhizobacteria and *acdS* rhizobacteria in the rhizosphere. On this basis, we tested here the hypothesis that rhizobacteria with either nitrogen fixation ability or ACC deamination ability (or with both) co-occur on roots. For that purpose, we used three maize fields under reduced nitrogen fertilization practices, with samplings carried out at 6-leaf and flowering stages during two consecutive years, and numbers of *nifH* and *acdS* rhizobacteria were monitored by

quantitative PCR. In addition, *nifH* and *acdS* rhizobacteria were assessed by metabarcoding (MiSeq Illumina sequencing) of *nifH* and *acdS* genes at one sampling, in parallel to sequencing of 16S rRNA genes for the whole rhizobacterial community.

2. MATERIALS AND METHODS

2.1. Field experiment

The experiment was conducted in 2014 and 2015 at field sites located in Chatonnay (L), Sérézin-de-la-Tour (FC) and Saint Savin (C), near the town of Bourgoin-Jallieu (Isère, France). According to the FAO soil reference base, L field corresponds to a luvisol, FC a fluvic cambisol and C a calcisol (Table 1). The trial set-up has been described in Rozier et al. (2017).

For each of the fields, the crop rotation consists in one year wheat, six years maize and one year rapeseed, and wheat was grown the year before the 2014 experiment. The maize sowing season ranges from middle April to middle May in the area. Maize seeds (*Zea mays* 'Seiddi'; Dauphinoise Company, France) were sown on April 18 (FC) and 23 (C and L) in 2014 and April 30 (C) and May 11 (FC and L) in 2015. Five replicate plots, which were 12 (FC and C) or 8 (L) maize rows wide and 12 m long, were defined in each field. The fields were undergoing a reduction in chemical fertilization usage and did not receive any nitrogen fertilizers in 2014 and 2015. Only non-inoculated plots from the overall trial (Rozier et al. 2017) were used.

2.2. Plant sampling

In 2014 and 2015, plants were sampled at six leaves and at flowering. In 2014, the first sampling was done on May 25 (FC) and 26 (C and L). On each replicate plot, six plants were chosen randomly, the entire root system was dug up and shaken vigorously to dislodge soil loosely

adhering to the roots. At sites FC and C, one pooled sample of six roots system was obtained per plot, i.e. a total of five pooled samples per field site. At site L, each of the six roots system was treated individually to obtain 30 samples. The second sampling was done on July 8 (FC and C) and 9 (L), on all five plots. Six plants were sampled per plot and treated individually to obtain 30 samples per field site.

In 2015, the first sampling was done on May 27 (C), June 5 (FC) and June 8 (L). In each replicate plot, four root systems were sampled and treated individually to obtain 20 samples per field site. The second sampling was done on July 15 (C), 16 (FC) and 17 (L), and four root systems were sampled and treated individually to obtain 20 samples per field site.

Each sample was immediately flash-frozen on site, in liquid nitrogen, and lyophilized back at the laboratory (at -50°C for 24 h). Roots and their adhering soil were separated and the latter stored at -80°C.

2.3. DNA extraction from root-adhering soil

DNA from root-adhering soil was extracted with the FastDNA SPIN kit (BIO 101 Inc., Carlsbad, CA). To this end, 500 mg (for the pooled samples from FC and C in 2014) or 300 mg samples (for all other samples) were transferred in Lysing Matrix E tubes from the kit, and 5 µl of the internal standard APA9 (10^9 copies ml^{-1}) was added to each Lysing Matrix E tube to normalize DNA extraction efficiencies between rhizosphere samples, as described (Park and Crowley, 2005; Couillerot et al. 2010). This internal standard APA9 (i.e. vector pUC19 with cassava virus insert; GenBank accession number AJ427910) requires primers AV1f (CACCATGTCGAAGCGACCAGGAGATATCATC) and AV1r (TTTCGATTTGTGACGTGGACAGTGGGGGC). After 1 h incubation at 4°C, DNA was extracted and eluted in 50 µl of sterile ultra-pure water, according to the manufacturer's instructions. DNA concentrations were assessed by Picogreen (ThermoFisher).

2.4. Size of microbial functional groups

The amounts of *nifH* genes were estimated by quantitative PCR based on the primers polF/polR (Poly, Jocteur Monrozier, and Bally, 2001), as described by Bouffaud et al. (2016). The reaction was carried out in 20 µl containing 4 µl of PCR-grade water, 1 µl of each primer (final concentration 0.50 µM), 10 µl of LightCycler-DNA Master SYBR Green I master mix (Roche Applied Science, Meylan, France) and 2 µl of sample DNA (10 µg). The cycling program included 10 min incubation at 95°C, followed by 50 cycles of 95°C for 15 s, 64°C for 15 s and 72°C for 10 s. Melting curve calculation and Tm determination were performed using the Tm Calling Analysis module of Light-Cycler Software v.1.5 (Roche Applied Science).

The amount of *acdS* genes was estimated by quantitative PCR based on the primers acdSF5/acdSR8 (Bouffaud et al. 2018). The reaction was carried out in 20 µl containing 4 µl of PCR grade water, 1 µl of each primer (final concentration 1 µM), 10 µl of LightCycler-DNA Master SYBR Green I master mix (Roche Applied Science) and 2 µl of sample DNA (10 µg). The cycling program included 10 min incubation at 95°C, followed by 50 cycles of 94°C for 15 s, 67°C for 15 s and 72°C for 10 s. The fusion program for melting curve analysis is described above.

Real-time PCR quantification data were converted to gene copy number per gram of lyophilized root-adhering soil, as described (Bouffaud et al. 2018; Bouffaud et al. 2016).

2.5. *nifH*, *acdS* and *rrs* sequencing from rhizosphere DNA

Sequencing was performed on 2015' samples taken when maize reached 6 leaves. Each sample was an equimolar composite sample of four DNA extracts obtained from root-adherent soil, resulting in 5 samples per field site, i.e. a total of 15 samples. DNA extracts were sent to MR DNA laboratory (www.mrdnalab.com; Shallowater, TX) for sequencing.

For *nifH* and *acdS* sequencing, PCR primers were the same ones used for quantitative PCR (i.e., polF/polR for *nifH* and acdSF5/acdSR8 for *acdS*). For *rrs* sequencing, PCR primers 515/806 were chosen for the V4 variable region of the 16S rRNA gene. For all three genes, the forward primer carried a barcode. Primers were used in a 30-cycle PCR (5 cycles implemented on PCR products), using the HotStarTaq Plus Master Mix Kit (Qiagen, Valencia, CA) under the following conditions: 94°C for 3 min, followed by 28 cycles of 94°C for 30 s, 53°C for 40 s and 72°C for 1 min, with a final elongation step at 72°C for 5 min. PCR products were checked in 2% agarose gel to determine amplification success and relative band intensity. Multiple samples were pooled together in equal proportions based on their molecular weight and DNA concentrations. Pooled samples were purified using calibrated Ampure XP beads and used to prepare a DNA library following Illumina TruSeq DNA library preparation protocol. Sequencing was performed on a MiSeq following the manufacturer's guidelines.

Sequence data were processed using the analysis pipeline of MR DNA. Briefly, sequences were depleted of barcodes, sequences < 150 bp or with ambiguous base calls removed, the remaining sequences denoised, operational taxonomic units (OTUs; defined at 3% divergence threshold for the three genes) generated, and chimeras removed. Final OTUs were taxonomically classified using BLASTn against a curated database derived from Greengenes (DeSantis et al. 2006), RDPII (http://rdp.cme.msu.edu) and NCBI (www.ncbi.nlm.nih.gov). Final OTUs of the *acdS* sequencing were classified using an in-house curated *acdS* database, obtained after curation of *acdS* homolog genes from the FunGene *acdS* 8.3 database, as described by Bouffaud et al. (2018). Diversity indices of Shannon (H) and Simpson (1-D) were calculated using sequencing subsample data for which each sample had the same number of sequences.

An *acdS* phylogenetic tree (based on maximum-likelihood method) was computed using *acdS* sequences from ten arbitrarily-chosen OTUs per genus recovered in our sequencing data

and from one reference taxa for each genus, and related D-cystein desulfhydrase genes D-cystein desulfhydrase genes from strains *Escherichia coli* strains K-12, ER3413, 042 and RM9387, *Escherichia albertii* KF1, *Escherichia fergusonii* ATCC 35469, *Enterobacter sacchari* SP1, *Enterobacter cloacae* ECNIH2, *Enterobacter asburiae* L1, *Enterobacter* sp. 638 and *Enterobacter lignolyticus* SCF1 (used as out-group).

2.6. Statistical analysis

Statistical analysis of quantitative PCR data was carried out by ANOVA and Fishers' LSD tests. For each gene sequenced, comparison of bacterial diversity between field sites was carried out by Between-Class Analysis (BCA) using ADE4 (Chessel et al. 2004; Culhane et al. 2005; Dray, Dufour, and Chessel, 2007) and ggplot2 packages for R, and the 12 genera contributing most to field site differentiation were identified. To assess co-trends between *nifH* and *acdS* variables, as well as between *rrs* and *nifH* or *acdS* variables, sequence data were also assessed using co-inertia analysis (CIA) (Dray et al. 2003; Dray et al. 2007), which was computed with the ADE4 package in the R statistical software environment (Culhane et al. 2005). CIA is a dimensional reduction procedure designed to measure the similarity of two sets of variables, here the proportions of *nifH* and *acdS* bacterial genera obtained during between-class analyses. Its significance was assessed using Monte-Carlo tests with 10,000 permutations. Unless otherwise stated, statistical analyses were performed using R v3.1.3 (Team, 2014), at $P < 0.05$ level.

2.7. Nucleotide sequence accession numbers

Illumina MiSeq paired-end reads have been deposited in the European Bioinformatics Institute (EBI) database under accession numbers PRJEB14347 (ERP015984) for *rrs*; PRJEB14346 (ERP015983) for *nifH*, PRJEB14343 (ERP015981) for *acdS*.

3. RESULTS

3.1. Relation between numbers of *nifH* and *acdS* alleles in the three field sites

The number of *acdS* bacteria in the rhizosphere of maize harvested at 6-leaf stage in 2014 (7.87 to 17.4 × 10^7 *acdS* gene copies g^{-1} of dry soil) and 2015 (1.76 to 2.81 × 10^7 *acdS* gene copies g^{-1} of dry soil) did not differ significantly between field sites (Figure 1AB). At flowering stage, however, the number of *acdS* bacteria differed from one site to the next, both in 2014 and in 2015 (Figure 1EF). At that growth stage, the lowest rhizosphere abundance was observed in site L (5.08 × 10^7 *acdS* gene copies g^{-1} of dry soil) and the highest in site C (1.76 × 10^8 *acdS* gene copies g^{-1} of dry soil) in 2014, whereas site ranking was the opposite in 2015 (8.35 versus 44.0 × 10^6 *acdS* gene copies g^{-1} of dry soil for sites C and L, respectively).

The numbers of *nifH* rhizobacteria differed according to field site (Figure 1CDGH). In 2014, the lowest *nifH* abundance was observed in rhizospheres of site L (1.06 and 20.8 × 10^7 *nifH* gene copies g^{-1} of dry soil at respectively six leaves and flowering) and the highest in those of site C (6.43 and 147.0 × 10^7 *nifH* gene copies g^{-1} of dry soil at respectively six leaves and flowering) (Figure 1CG). In 2015, the numbers of *nifH* rhizobacteria was higher in site C (9.31 × 10^8 *nifH* gene copies g^{-1} of dry soil) than in FC (1.30 × 10^8 *nifH* gene copies g^{-1} of dry soil) and L (2.52 × 10^8 *nifH* gene copies g^{-1} of dry soil) at six leaves, whereas the situation was opposite at flowering, with higher abundance in site L (40.7 × 10^7 *nifH* gene copies g^{-1} of dry soil) than C (9.81 × 10^7 *nifH* gene copies g^{-1} of dry soil) and FC (5.66 × 10^7 *nifH* gene copies g^{-1} of dry soil) (Figure 1DH).

When comparing the log numbers of *nifH* rhizobacteria and *acdS* rhizobacteria across the 12 site × sampling combinations, significant ($3.8 \times 10^{-5} < P < 0.01$) positive correlations ($0.67 < r < 0.98$, $n = 20$) were found in 9 of 12 cases, with only three correlations that were not

significant, i.e. in site C at 6-leaf stage in 2014 (P = 0.10, n = 5) and FC at flowering in 2014 (P = 0.67, n = 5) and 2015 (P = 0.19, n = 20) (Figure 2). In summary, moderate but significant differences in the numbers of *nifH* and/or *acdS* rhizobacteria could take place according to field site, sampling year and/or maize phenology, and in most cases a positive correlation was found between the log values of both numbers.

3.2. Relation between diversities of *nifH* and *acdS* alleles in the three field sites

Illumina MiSeq sequencing of *nifH* and *acdS* (as well as *rrs*) was carried out on 15 rhizosphere samples from 6-leaf maize grown in 2015. For *nifH*, 1,342,966 reads were obtained (10,775 to 62,752 sequences per sample), for a total of 36,241 OTUs. Rarefaction analysis showed that curves reached a plateau (Figure S1A). Subsampling was done with 10,775 sequences per sample, for a total of 34,459 OTUs. For *acdS*, 5,490,230 reads were obtained (68,376 to 139,245 sequences per sample), with a total of 32,468 OTUs. Rarefaction curves reached a plateau (Figure S1B). Subsampling was done with 68,376 sequences per sample, for a total of 26,246 OTUs. After quality filtering, 6,082,255 reads were obtained for *rrs* (51,696 to 223,926 sequences per sample), giving a total of 39,600 OTUs (3% cut-off). Rarefaction analysis showed that the sequencing effort captured most of the diversity with curves reaching a plateau (Figure S1C). Subsampling was done with 51,696 sequences per sample, for a total of 25,437 OTUs.

The effect of field site on *nifH* diversity of diazotrophic bacteria was not significant based on analysis of Shannon and Simpson indices. Conversely, the effect of field site on *acdS* diversity of ACC deaminase bacteria was significant based on the Shannon ($P = 1.9. \times 10^{-4}$) and Simpson indices ($P = 8.6 \times 10^{-4}$). The Shannon index was lower in FC (6.32) than in L (6.82) and C (6.92), whereas the Simpson index was higher in FC (6.42×10^{-3}) than in L (2.88×10^{-3}) and C (2.38×10^{-3}). The effect of field site on *rrs* diversity of the total bacterial

community was significant based on the Shannon ($P = 1.8 \times 10^{-5}$) and Simpson indices ($P = 1.6 \times 10^{-4}$). As in the case of *acdS* data, the Shannon index was lower in FC (7.20) than in L (7.41) and C (7.71), whereas the Simpson index was higher in FC (3.42×10^{-3}) than in L (2.28×10^{-3}) and C (1.40×10^{-3}).

The correlation (n = 5) between *nifH* diversity and *acdS* diversity was positive and significant at site L, when considering both the Shannon index (r = 0.98 ; $P = 0.01$; Figure 3) and the Simpson index (r = 0.86 ; $P = 0.06$; Figure 3). However, the correlation was not significant at the other two sites, regardless of the diversity index. When considering also *rrs* diversity, a significant correlation was found only with *nifH* diversity at site C (r = 0.91 ; $P = 0.03$; Figure 3). In summary, there was no relation between the diversities of *nifH* rhizobacteria and *acdS* rhizobacteria, based on comparison of diversity indices in the three field sites and correlation analyses at two of the three field sites.

3.3. Relation between prevalence of *nifH* and/or *acdS* rhizobacterial taxa in the three field sites

Between-class analysis of *nifH* data showed that the composition of diazotrophic bacteria differed according to field site (Figure 4A). The first axis (54% of between-class variability) distinguished site C from FC and L, and the 12 genera contributing most to this differentiation were *Xanthobacter, Dechloromonas, Methyloferula, Ideonella, Nitrospirillum* and *Tolumonas* (more prevalent in C than in L and FC), as well as *Desulfovibrio, Selenomonas, Ruminiclostridium, Paludibacter, Gloeocapsopsis* and *Ruminococcus* (less prevalent in C than in FC and L). The second axis (46% of between-class variability) distinguished site L from the two other sites, and the 12 genera contributing most to this differentiation included *Rhizobium, Gluconacetobacter, Skermanella, Leptothrix, Streptomyces* and *Methylocapsa* (more prevalent in L than in FC and C), as well as *Marichromatium, Pelobacter, Gordonibacter, Desulfobulbus, Desulfovibrio* and *Sideroxydan* (less prevalent in L than in C and FC).

Between-class analysis of *acdS* data showed that the composition of ACC deaminase bacteria differed according to field site (Figure 4B). The first axis (66% of between-class variability) distinguished site C from FC and L, and the 12 genera contributing most to this differentiation were *Achromobacter, Azospirillum, Pseudolabrys, Roseovarius,* one unassigned OTU and *Polaromonas* (more prevalent in C than in L and FC), as well as *Cupriavidus, Burkholderia, Bosea, Bradyrhizobium* and *Methylobacterium* (less prevalent in C than in FC and L). The second axis (34% of between-class variability) distinguished each of the three sites from one another, and the 12 genera contributing most to this differentiation included *Azorhizobium, Pseudomonas, Gluconobacter, Collimonas, Herbaspirillum* and *Burkholderia* (more prevalent in FC than in C and L), as well as *Ralstonia, Loktanella, Devosia, Variovorax, Novosphingobium* and *Chelatococcus* (more prevalent in L than in C and FC).

Between-class analysis of *rrs* data showed that the composition of the total bacterial community differed according to field site (Figure 4C). The first axis (71% of between-class variability) distinguished C from the two other sites, and the 12 genera contributing most to this differentiation were *Algisphaera, Fibrobacter, Amaricoccus, Hirschia, Desulfacinum* and *Saccharophagus* (more prevalent in C than in L and FC), as well as *Actinomadura, Lutispora, Bacillus, Rhodopseudomonas, Kouleothrix* and *Roseiflexus* (less prevalent in C than in FC and L). The second axis (29% of between-class variability) distinguished site L from FC and C, and the 12 genera contributing most to this differentiation included *Flavobacterium, Gluconobacter, Maricaulis, Prolixibacter, 'Candidatus* Xiphinematobacter', *Chthoniobacter* (more prevalent in FC than L), as well as *Conexibacter, Hyphomicrobium, Pseudonocardia, Tumebacillus, Chelatococcus* and *Mycobacterium* (less prevalent in FC than in L).

In summary, between-class analysis of *nifH* and *acdS* data indicated that the composition of diazotrophic bacteria and of ACC deaminase bacteria differed according to field site, but the main discriminant genera differed completely for both types of bacteria. In both cases, the discriminant taxa were also different from the main range of bacterial taxa distinguishing the three sites most when comparing the latter based on *rrs* data, at the scale of the entire rhizobacterial community.

3.4. Relation between the genetic structures of *nifH* and *acdS* rhizobacteria in the three field sites

Since there was a positive correlation between log numbers of *nifH* and/or *acdS* rhizobacteria but the corresponding bacterial genera discriminating most between the three fields studied were not the same, the co-structuration between *nifH* and *acdS* diversity was explored by co-inertia analysis to compare more globally the genetic structures of these rhizobacterial groups across the three field sites. Monte-Carlo permutation tests showed a significant co-structuration

($P = 9 \times 10^{-5}$) of *nifH* and *acdS* rhizobacteria, with a RV coefficient of 0.83. This accounted for 57% of data variability. The plot of the co-inertia matrix illustrates the strength of the relationship between *acdS* and *nifH* diversities, as superposition of *acdS* and *nifH* groups showed a strong co-trend in all three field sites (Figure 5).

Co-inertia analyses of *nifH* and *acdS* diversities were also performed with *rrs* diversity, and permutations tests also showed co-structuration in both cases, with respectively RV coefficients of 0.89 and 0.91, the two axes explaining 52% and 69% of variability. Superposition of *rrs* community with *acdS* and with *nifH* groups indicated a strong co-trend across the three fields.

In summary, the genetic structures of *nifH* and *acdS* rhizobacterial groups across the three field sites were very close. Co-inertia was strong also when comparing each with the whole rhizobacterial community based on *rrs* data.

4. DISCUSSION

The current work made use of molecular tools available to characterize functional groups of *nifH* and *acdS* bacteria. Quantification of *nifH* rhizobacteria was performed with primers PolF/PolR (Poly et al. 2001) rather than other well-established primers such as Zf/Zr (Zehr and McReynolds, 1989) since the latter are not effective for quantitative PCR (Boyd and Peters 2013; Gaby and Buckley 2017; Poly et al. 2001). The same primers have also been used for sequencing, both for consistency and efficacy for diazotroph characterization (Mårtensson et al. 2009; Wartiainen et al. 2008). Recently, *acdS* primers suitable for monitoring of ACC deamination bacteria have been made available (Bouffaud et al. 2018). These primers are effective to amplify true *acdS* genes while not amplifying related D-cystein desulfhydrase genes coding for other PLP-dependent enzymes, which was verified again in the current work (Figure

S2). Indeed, phylogenetic analysis of the *acdS* sequences showed that none clustered within the out-group (built with strains harboring D-cystein desulfhydrase genes), confirming that the sequences obtained were true *acdS* sequences, as highlighted in previous studies (Blaha et al. 2006; Bouffaud et al. 2018; Li et al. 2015; Nascimento et al. 2012).

The level of taxonomic information carried by *nifH* sequences has been described in the literature, showing that *nifH* was sufficiently conserved to enable reliable taxonomic affiliations including for the assessment of rhizobacteria (Vinuesa et al. 2005), and its phylogeny was congruent with the one derived from *rrs* (Achouak et al. 1999; Zehr et al. 2003). As for *acdS*, phylogenetic analysis of the new sequences obtained (along with reference *acdS* sequences) confirmed that the taxonomic affiliations made at the genus level were correct. However, the 130-bp *acdS* amplicons obtained with the current quantitative PCR primers do not enable any taxonomic affiliation below the genus level, i.e. at the species level (Bouffaud et al. 2018).

In this work, the hypothesis that *nifH* and *acdS* rhizobacterial populations co-occur on roots was assessed with maize taken from three fields, using quantitative PCR and MiSeq sequencing. The results that were obtained did substantiate this hypothesis, based on (i) positive correlations between the sizes of *nifH* and *acdS* rhizobacterial groups, and (ii) comparable genetic structures indicated by inertia analysis for both functional groups across the three field sites studied. Several studies have assessed the co-occurrence of particular microorganisms and measured between-taxa correlations in soil systems (Barberán et al. 2011; Freilich et al. 2010), but few have done so at the level of functional groups. For instance, co-occurrence analysis of nitrite-dependent anaerobic ammonium oxidizers and methane oxidizers in paddy soil showed that the structure of these communities changed with soil depth (Wang et al. 2012). The co-occurrence of plant-beneficial functions in the rhizosphere has been investigated, but often the assessment was restrained to narrow taxonomic levels, such as within the *Pseudomonas* genus (Almario et al. 2014; Frapolli et al. 2012; Vacheron et al. 2016). It is interesting to note that not

all microorganisms harboring *acdS* and/or *nifH* expressed the corresponding functions in rhizosphere based on assessment of qRT-PCR data, as previously described for *nifH* (Bouffaud et al. 2016) or *acdS* (Bouffaud et al. 2018).

Specific taxa can be selected by environmental conditions prevailing on plant roots (Bakker et al. 2014; Berg and Smalla, 2009; Raaijmakers et al. 2009; Vandenkoornhuyse et al. 2015). Thus, a first possibility to account for the co-occurrence of both functional groups could be that both *nifH* bacteria and *acdS* bacteria do well in the maize rhizosphere. Indeed, both types of bacteria are readily found on roots (Almario et al. 2014; Arruda et al. 2013; Blaha et al. 2006; Bruto et al. 2014; Bruto et al. 2014; Mårtensson et al. 2009). Such co-occurrence would make sense in ecological terms, because associative nitrogen fixation and ACC deamination are functions limiting plant nutrient deficiency by supplying nitrogen (Pii et al. 2015) and enhancing root system development (thereby improving uptake of mineral nutriments including nitrogen) (Glick, 2014), respectively.

A second possibility could be that bacteria that harbor both genes/functions are well adapted to maize roots. Indeed, Bruto et al. (2014) showed that the *nif* operon co-occurred with *acdS* in several bacterial clades, and for instance the genera *Bradyrhizobium* or *Burkholderia* contain several species harboring both functions (Bruto et al. 2014). Furthermore, the co-inertia between these two functional groups and the total community raises the possibility that additional functions could also be present in addition to associative nitrogen fixation and ACC deamination. Indeed, comparative genomics studies showed that bacterial taxa display multiple specific functions, including plant interaction functions (Bruto et al. 2014; Lassalle et al. 2015; Vacheron et al. 2017), and thus these functions would also be co-selected when selecting the corresponding *rrs*-based taxa. In the current study, *Bradyrhizobium* represented 17 to 25% of *acdS*$^+$ bacteria and 20 to 42% of *nifH*$^+$ bacteria in the maize rhizosphere, and the high proportion of this bacterial clade may contribute to the co-occurence of diazotrophs and ACC deaminase

producers that was found. However, when the 10,369 completely-sequenced bacterial genomes available in the NCBI database were screened, it showed that 833 of them harbored *acdS* and 461 others *nifH*, but only 122 genomes had both genes. Therefore, it could be that this second possibility is insufficient for a complete explanation of the current findings.

A third possibility to consider is the joint occurrence of both functions in the rhizosphere, regardless of the taxa harboring them, thereby providing functional redundancy (Shade and Handelsman, 2012). Several studies in soil or aquatic settings have suggested that the metabolic/functional potential of microbial communities rather than their taxonomic variations are closely related to environmental conditions (Bouffaud et al. 2018; Burke et al. 2011; Louca et al. 2016; Louca et al. 2017). These observations were conceptualized as the "It's the song, not the singer" theory (ITSNTS; Doolittle and Booth 2017), i.e. functional groups within microbial communities (the songs) would be better conserved and more relevant ecologically than the taxa themselves (the singers). Consistent with the ITSNTS theory, our study suggests that the assembly of the rhizosphere microbial community would entail a balance between phytostimulation-relevant genes, which may be needed to achieve an effective holobiont (i.e., the plant host and its functional microbiota), and points to the preponderance of functional interactions within the plant holobiont. This hypothesis, which has been put forward recently for root-associated microorganisms (Lemanceau et al. 2017), remains speculative at this stage and deserves further research attention. In particular, methodology development is needed to enable direct assessment of key plant-beneficial groups when parallel monitoring of several genes is required (e.g. for auxin production or P solubilization, which entail many genetic pathways), in contrast to ACC deamination and N fixation for which analysis of a single gene (*acdS* and *nifH*, respectively) may suffice.

To test whether the current findings could be also relevant under other environmental conditions, we reassessed the data obtained for *nifH* (Bouffaud et al. 2016) and *acdS* (Bouffaud

et al. 2018) from two maize lines grown in another soil (luvisol) with different management histories (cropped soil vs meadow soil). A positive correlation (r = 0.45 ; P = 0.050 ; n = 20) was found between the numbers of *nifH* and *acdS* bacteria in the monocropping soil but not in meadow soil (P = 0.75 ; n = 10), suggesting that maize monocropping history could have been an important factor. However, these findings were obtained with young plants only (21 days), grown in sieved soil under greenhouse conditions.

In conclusion, the current findings indicate that rhizobacteria with nitrogen fixation capacity and counterparts harboring ACC deamination ability co-occur in the maize rhizosphere, pointing to the possibility that plants may rely on multiple, complementary phytostimulatory functions provided by their microbial partners. Additional method development is needed to extend this type of assessment to additional phytostimulatory groups and other microbial functional groups important for plant performance.

ACKNOWLEDGEMENTS

This work was supported in part by project Azodure (ANR Agrobiosphère ANR-12-AGRO-0008). We are grateful to J. Haurat and H. Brunet for technical help, as well as D. Abrouk (iBio platform, UMR CNRS 5557 Écologie Microbienne) and J. Thioulouse (UMR CNRS LBBE) for helpful discussion. The authors declare no conflict of interest.

DATA ACCESSIBILITY

Illumina MiSeq paired-end reads have been deposited in the European Bioinformatics Institute (EBI) database under accession numbers PRJEB14347 (ERP015984) for *rrs*; PRJEB14346 (ERP015983) for *nifH*, PRJEB14343 (ERP015981) for *acdS*.

AUTHOR CONTRIBUTIONS

LL, YML and DM designed the project, SR, LL, CPC, YML and DM carried out field work and samplings, SR conducted the molecular work, SR, MLB and AD implemented bioinformatic analyses, SR, YML and DM analyzed data, SR, YML and DM prepared the first draft of the manuscript, which was finalized by all authors.

REFERENCES

Achouak W, Normand P, Heulin T. Comparative phylogeny of *rrs* and *nifH* genes in the *Bacillaceae*. *Int J Syst Evol Microbiol* 1999;*49*(3):961-967. doi:10.1099/00207713-49-3-961

Agaras BC, Scandiani M, Luque A *et al.* Quantification of the potential biocontrol and direct plant growth promotion abilities based on multiple biological traits distinguish different groups of *Pseudomonas* spp. isolates. *Biological Control* 2015;*90*:173-186. doi:https://doi.org/10.1016/j.biocontrol.2015.07.003

Almario J, Gobbin D, Défago G *et al.* Prevalence of type III secretion system in effective biocontrol pseudomonads. *Res Microbiol* 2014;*165*(4):300-304. doi:https://doi.org/10.1016/j.resmic.2014.03.008

Almario J, Muller D, Défago G *et al.* Rhizosphere ecology and phytoprotection in soils naturally suppressive to Thielaviopsis black root rot of tobacco. *Environ Microbiol* 2014;*16*(7):1949-1960. doi:10.1111/1462-2920.12459

Arruda L, Beneduzi A, Martins A *et al.* Screening of rhizobacteria isolated from maize (*Zea mays* L.) in Rio Grande do Sul State (South Brazil) and analysis of their potential to improve plant growth. *Appl Soil Ecol* 2013;*63*:15-22. doi:https://doi.org/10.1016/j.apsoil.2012.09.001

Bakker MG, Schlatter DC, Otto-Hanson L *et al.* Diffuse symbioses: roles of plant–plant, plant–microbe and microbe–microbe interactions in structuring the soil microbiome. *Mol Ecol* 2014;*23*(6):1571-1583. doi:10.1111/mec.12571

Barberán A, Bates ST, Casamayor EO *et al.* Using network analysis to explore co-occurrence patterns in soil microbial communities. *ISME J* 2011;*6*:343–351. doi:10.1038/ismej.2011.119 https://www.nature.com/articles/ismej2011119#supplementary-information

Bashan Y, de-Bashan LE. Chapter Two - How the plant growth-promoting bacterium *Azospirillum* promotes plant growth—A critical assessment. In: Sparks DL (ed). *Advances in Agronomy*. Academic Press, 2010, 108, 77-136.

Bashan Y, de-Bashan LE, Prabhu SR *et al.* Advances in plant growth-promoting bacterial inoculant technology: formulations and practical perspectives (1998–2013). *Plant Soil* 2014;*378*(1):1-33. doi:10.1007/s11104-013-1956-x

Berg G, Smalla K. Plant species and soil type cooperatively shape the structure and function of microbial communities in the rhizosphere. *FEMS Microbiol Ecol* 2009;*68*(1):1-13. doi:10.1111/j.1574-6941.2009.00654.x

Bertalan M, Albano R, de Pádua V *et al.* Complete genome sequence of the sugarcane nitrogen-fixing endophyte *Gluconacetobacter diazotrophicus* Pal5. *BMC Genomics* 2009;*10*(1):450. doi:10.1186/1471-2164-10-450

Blaha D, Prigent-Combaret C, Mirza MS *et al.* Phylogeny of the 1-aminocyclopropane-1-carboxylic acid deaminase-encoding gene *acdS* in phytobeneficial and pathogenic Proteobacteria and relation with strain biogeography. *FEMS Microbiol Ecol* 2006;*56*(3):455-470. doi:10.1111/j.1574-6941.2006.00082.x

Bouffaud M-L, Renoud S, Dubost A *et al.* 1-Aminocyclopropane-1-carboxylate deaminase producers associated to maize and other Poaceae species. *Microbiome* 2018;*6*(1):114. doi:10.1186/s40168-018-0503-7

Bouffaud M-L, Renoud S, Moënne-Loccoz Y *et al.* Is plant evolutionary history impacting recruitment of diazotrophs and *nifH* expression in the rhizosphere? *Sci Rep* 2016;*6*:21690. doi:10.1038/srep21690 http://www.nature.com/articles/srep21690#supplementary-information

Boyd E, Peters J. New insights into the evolutionary history of biological nitrogen fixation. *Front Microbiol* 2013;*4*:201. doi:10.3389/fmicb.2013.00201

Bruto M, Prigent-Combaret C, Luis P *et al.* Frequent, independent transfers of a catabolic gene from bacteria to contrasted filamentous eukaryotes. *Proc R Soc Lond B: Biol Sci* 2014;*281*:1789. doi:10.1098/rspb.2014.0848

Bruto M, Prigent-Combaret C, Muller D *et al.* Analysis of genes contributing to plant-beneficial functions in plant growth-promoting rhizobacteria and related Proteobacteria. *Sci Rep* 2014;*4*:6261. doi:10.1038/srep06261

Burke C, Steinberg P, Rusch D *et al.* Bacterial community assembly based on functional genes rather than species. *Proc Natl Acad Sci USA* 2011;*108*(34):14288-14293. doi:10.1073/pnas.1101591108

Cassán F, Vanderleyden J, Spaepen S. Physiological and agronomical aspects of phytohormone production by model Plant-Growth-Promoting Rhizobacteria (PGPR) belonging to the genus *Azospirillum*. *J. Plant Growth Regul* 2014;*33*(2):440-459. doi:10.1007/s00344-013-9362-4

Chen XH, Koumoutsi A, Scholz R *et al.* Comparative analysis of the complete genome sequence of the plant growth–promoting bacterium *Bacillus amyloliquefaciens* FZB42. *Nature Biotechnol* 2007;*25*:1007. doi:10.1038/nbt1325 https://www.nature.com/articles/nbt1325#supplementary-information

Chessel D, Dufour AB, Thioulouse J. The ade4 package-I-One-table methods. *R News* 2004;*4*(1):5-10.

Cormier F, Foulkes J, Hirel B *et al.* Breeding for increased nitrogen-use efficiency: a review for wheat (*T. aestivum* L.). *Plant Breeding* 2016;*135*(3):255-278. doi:10.1111/pbr.12371

Couillerot O, Ramírez-Trujillo A, Walker V *et al.* Comparison of prominent *Azospirillum* strains in *Azospirillum–Pseudomonas–Glomus* consortia for promotion of maize growth. *Appl Microbiol Biotechnol* 2013;*97*(10):4639-4649. doi:10.1007/s00253-012-4249-z

Culhane AC, Thioulouse J, Perrière G *et al.* MADE4: an R package for multivariate analysis of gene expression data. *Bioinformatics* 2005;*21*(11):2789-2790. doi:10.1093/bioinformatics/bti394

Deynze A, Zamora P, Delaux P-M *et al.* Nitrogen fixation in a landrace of maize is supported by a mucilage-associated diazotrophic microbiota. *PLoS Biol* 2018;*16*(8):e2006352. https://doi-org.inee.bib.cnrs.fr/10.1371/journal.pbio.2006352

DeSantis TZ, Hugenholtz P, Larsen N *et al.* Greengenes, a chimera-checked 16S rRNA gene database and workbench compatible with ARB. *Appl Environ Microbiol* 2006;*72*(7):5069-5072. doi:10.1128/aem.03006-05

Doolittle WF, Booth A. It's the song, not the singer: an exploration of holobiosis and evolutionary theory. *Biol Philos* 2017;*32*(1):5-24. doi:10.1007/s10539-016-9542-2

Dray S, Chessel D, Thioulouse J. Co-inertia analysis and the linking of ecological data tables. *Ecology* 2003;*84*(11):3078-3089. doi:10.1890/03-0178

Dray S, Dufour AB, Chessel D. The ade4 Package—II: Two-table and K-table methods. *R News* 2007;*7*:47-52.

Duan J, Müller KM, Charles T *et al.* 1-aminocyclopropane-1-carboxylate (ACC) deaminase genes in Rhizobia from southern Saskatchewan. *Microb Ecol* 2009;*57*(3):423-436. doi:10.1007/s00248-008-9407-6

Frapolli M, Pothier JF, Défago G *et al.* Evolutionary history of synthesis pathway genes for phloroglucinol and cyanide antimicrobials in plant-associated fluorescent pseudomonads. *Mol Phylogenet Evol* 2012;*63*(3):877-890. doi:https://doi.org/10.1016/j.ympev.2012.02.030

Freilich S, Kreimer A, Meilijson I *et al.* The large-scale organization of the bacterial network of ecological co-occurrence interactions. *Nucleic Acids Res* 2010;*38*(12):3857-3868. doi:10.1093/nar/gkq118

Gaby JC, Buckley DH. The use of degenerate primers in qPCR analysis of functional genes can cause dramatic quantification bias as revealed by investigation of *nifH* primer performance. *Microb Ecol* 2017;*74*(3):701-708. doi:10.1007/s00248-017-0968-0

Gamalero E, Glick BR. Bacterial modulation of plant ethylene levels. *Plant Physiol* 2015;*169*(1):13-22. doi:10.1104/pp.15.00284

Glick BR. Bacteria with ACC deaminase can promote plant growth and help to feed the world. *Microbiol Res* 2014;*169*(1):30-39. doi:https://doi.org/10.1016/j.micres.2013.09.009

Hartman K, van der Heijden MGA, Wittwe RA *et al.* Cropping practices manipulate abundance patterns of root and soil microbiome members paving the way to smart farming. *Microbiome* 2018;*6*(1):14. doi:10.1186/s40168-017-0389-9

Jha B, Gontia I, Hartmann A. The roots of the halophyte *Salicornia brachiata* are a source of new halotolerant diazotrophic bacteria with plant growth-promoting potential. *Plant Soil* 2012;*356*(1):265-277. doi:10.1007/s11104-011-0877-9

Lassalle F, Muller D, Nesme X. Ecological speciation in bacteria: reverse ecology approaches reveal the adaptive part of bacterial cladogenesis. *Res Microbiol* 2015;*166*(10):729-741. doi:https://doi.org/10.1016/j.resmic.2015.06.008

Lemanceau P, Blouin M, Muller D, *et al.* Let the core microbiota be functional. *Trends Plant Sci* 2017;*22*(7):583-595. doi:https://doi.org/10.1016/j.tplants.2017.04.008

Li Z, Chang S, Ye S *et al.* Differentiation of 1-aminocyclopropane-1-carboxylate (ACC) deaminase from its homologs is the key for identifying bacteria containing ACC deaminase. *FEMS Microbiol Ecol* 2015;*91*(10):fiv112-fiv112. doi:10.1093/femsec/fiv112

Louca S, Parfrey LW, Doebeli M. Decoupling function and taxonomy in the global ocean microbiome. *Science* 2016;*353*(6305):1272-1277. doi:10.1126/science.aaf4507

Louca S, Jacques SMS, Pires APF *et al.* High taxonomic variability despite stable functional structure across microbial communities. *Nat Ecol Evol* 2017;*1*:0015. doi:10.1038/s41559-016-0015

Ma W, Guinel FC, Glick, BR. *Rhizobium leguminosarum* biovar *viciae* 1-aminocyclopropane-1-carboxylate deaminase promotes nodulation of pea plants. *Appl Environ Microbiol* 2003;*69*(8):4396-4402. doi:10.1128/aem.69.8.4396-4402.2003

Mårtensson L, Díez B, Wartiainen I *et al.* Diazotrophic diversity, *nifH* gene expression and nitrogenase activity in a rice paddy field in Fujian, China. *Plant Soil* 2009;*325*(1):207-218. doi:10.1007/s11104-009-9970-8

Nascimento FX, Brígido C, Glick BR *et al.* ACC deaminase genes are conserved among *Mesorhizobium* species able to nodulate the same host plant. *FEMS Microbiol Lett* 2012;*336*(1):26-37. doi:10.1111/j.1574-6968.2012.02648.x

Nukui N, Minamisawa K, Ayabe S-I *et al.* Expression of the 1-aminocyclopropane-1-carboxylic acid deaminase gene requires symbiotic nitrogen-fixing regulator gene *nifA2* in *Mesorhizobium loti* MAFF303099. *Appl Environ Microbiol* 2006;*72*(7):4964-4969. doi:10.1128/aem.02745-05

Pieterse CMJ, Van Wees SCM. Induced disease resistance. In: Lugtenberg B (ed). *Principles of Plant-Microbe Interactions: Microbes for Sustainable Agriculture*. Springer International Publishing, 2015, 123-33.

598 Pii Y, Mimmo T, Tomasi N *et al.* Microbial interactions in the rhizosphere: beneficial influences of
599 plant growth-promoting rhizobacteria on nutrient acquisition process. A review. *Biol Fertil*
600 *Soils* 2015;*51*(4):403-415. doi:10.1007/s00374-015-0996-1
601 Poly F, Jocteur Monrozier L, Bally R. Improvement in the RFLP procedure for studying the diversity
602 of *nifH* genes in communities of nitrogen fixers in soil. *Res Microbiol* 2001;*152*(1):95-103.
603 doi:https://doi.org/10.1016/S0923-2508(00)01172-4
604 Prigent-Combaret C, Blaha D, Pothier J *et al.* Physical organization and phylogenetic analysis of *acdR*
605 as leucine-responsive regulator of the 1-aminocyclopropane-1-carboxylate deaminase gene
606 *acdS* in phytobeneficial *Azospirillum lipoferum* 4B and other *Proteobacteria*. *FEMS*
607 *Microbiol Ecol* 2008;*65*(2):202-219. doi:10.1111/j.1574-6941.2008.00474.x
608 Puri A, Padda KP, Chanway CP. Evidence of nitrogen fixation and growth promotion in canola
609 (*Brassica napus* L.) by an endophytic diazotroph *Paenibacillus polymyxa* P2b-2R. *Biol Fertil*
610 *Soils* 2016;*52*(1):119-125. doi:10.1007/s00374-015-1051-y
611 Raaijmakers JM, Paulitz TC, Steinberg C *et al.* The rhizosphere: a playground and battlefield for
612 soilborne pathogens and beneficial microorganisms. *Plant Soil* 2009;*321*(1):341-361.
613 doi:10.1007/s11104-008-9568-6
614 Rana A, Saharan B, Joshi M *et al*. Identification of multi-trait PGPR isolates and evaluating their
615 potential as inoculants for wheat. *Ann Microbiol* 2011;*61*(4):893-900. doi:10.1007/s13213-
616 011-0211-z
617 Redondo-Nieto M, Barret M, Morrissey J *et al.* Genome sequence reveals that *Pseudomonas*
618 *fluorescens* F113 possesses a large and diverse array of systems for rhizosphere function and
619 host interaction. *BMC Genomics* 2013;*14*(1):54. doi:10.1186/1471-2164-14-54
620 Rozier C, Hamzaoui J, Lemoine D *et al.* Field-based assessment of the mechanism of maize yield
621 enhancement by *Azospirillum lipoferum* CRT1. *Sci Rep* 2017;*7*(1):7416. doi:10.1038/s41598-
622 017-07929-8
623 Shade A, Handelsman J. Beyond the Venn diagram: the hunt for a core microbiome. *Environ*
624 *Microbiol* 2012;*14*(1):4-12. doi:10.1111/j.1462-2920.2011.02585.x

Team, R. *R: A Language and Environment for Statistical Computing* 2014. Vienna, Austria: R Foundation for Statistical Computing.

Vacheron J, Desbrosses G, Bouffaud M-L *et al.* Plant growth-promoting rhizobacteria and root system functioning. *Front Plant Sci* 2013;*4*:356. doi:10.3389/fpls.2013.00356

Vacheron J, Desbrosses G, Renoud S *et al.* Differential contribution of plant-beneficial functions from *Pseudomonas kilonensis* F113 to root system architecture alterations in *Arabidopsis thaliana* and *Zea mays*. *Mol Plant-Microbe Interact* 2017;*31*(2):212-223. doi:10.1094/MPMI-07-17-0185-R

Vacheron J, Moënne-Loccoz Y, Dubost A *et al.* Fluorescent *Pseudomonas* strains with only few plant-beneficial properties are favored in the maize rhizosphere. *Front Plant Sci* 2016;*7*:1212. doi:10.3389/fpls.2016.01212

Vandenkoornhuyse P, Quaiser A, Duhamel *et al.* The importance of the microbiome of the plant holobiont. *New Phytol* 2015;*206*(4):1196-1206. doi:doi:10.1111/nph.13312

Vinuesa P, Silva C, Lorite MJ *et al.* Molecular systematics of rhizobia based on maximum likelihood and Bayesian phylogenies inferred from *rrs*, *atpD*, *recA* and *nifH* sequences, and their use in the classification of *Sesbania* microsymbionts from Venezuelan wetlands. *Syst Appl Microbiol* 2005;*28*(8):702-716. doi:https://doi.org/10.1016/j.syapm.2005.05.007

Wang Y, Zhu G, Harhangi HR *et al.* Co-occurrence and distribution of nitrite-dependent anaerobic ammonium and methane-oxidizing bacteria in a paddy soil. *FEMS Microbiol Lett* 2012;*336*(2):79-88. doi:10.1111/j.1574-6968.2012.02654.x

Wartiainen I, Eriksson T, Zheng W *et al.* Variation in the active diazotrophic community in rice paddy—*nifH* PCR-DGGE analysis of rhizosphere and bulk soil. *Appl Soil Ecol* 2008;*39*(1):65-75. doi:https://doi.org/10.1016/j.apsoil.2007.11.008

Wisniewski-Dyé F, Lozano L, Acosta-Cruz E *et al.* Genome sequence of *Azospirillum brasilense* CBG497 and comparative analyses of *Azospirillum* core and accessory genomes provide insight into niche adaptation. *Genes* 2012;*3*(4):576.

Zehr JP, Jenkins BD, Short SM *et al.* Nitrogenase gene diversity and microbial community structure: a cross-system comparison. *Envirol Microbiol* 2003;*5*(7):539-554. doi:10.1046/j.1462-2920.2003.00451.x

Zehr JP, McReynolds LA. Use of degenerate oligonucleotides for amplification of the *nifH* gene from the marine cyanobacterium *Trichodesmium thiebautii*. *Appl Environ Microbiol* 1989;*55*(10):2522-2526.

Legend

FIGURE 1. Size of the *acdS* and *nifH* functional groups compared in the three field sites L, FC and C over four sampling times. Means and standard deviations are shown for the *acdS* group at 6 leaves in 2014 (A) and 2015 (B) and at flowering in 2014 (E) and 2015 (F) and for the *nifH* group at 6 leaves in 2014 (C) and 2015 (D) and at flowering in 2014 (G) and 2015 (H). The analysis was done using pooled samples of six roots systems (n= 5) at FC and C and individual root systems (n = 30) at L in 2014, and individual root systems (n = 20) at all three sites in 2015. Statistical differences between sites are indicated by letters a-c (ANOVA and Fischer's LSD tests, $P < 0.05$).

FIGURE 2. Correlation between log numbers of *nifH* (X axis) and *acdS* genes (Y axis). Correlation was established using the Pearson coefficient. The analysis was done using pooled samples of six roots systems (n= 5) at FC and C and individual root systems (n = 30) at L in 2014, and individual root systems (n = 20) at all three sites in 2015.

FIGURE 3. Correlation between Shannon diversity indices of *nifH* and *acdS* (A), Simpson diversity indices of *nifH* and *acdS* (B), Shannon diversity indices of *rrs* and *acdS* or *nifH* (C), and Simpson diversity indices of *rrs* and *acdS* or *nifH* (D). Correlation was established separately at each of the three field sites L, FC and C, using the Pearson coefficient (n = 5).

FIGURE 4. Comparison of *nifH* (A), *acdS* (B) and *rrs* (C) diversity between sites L, FC and C by between-class analysis. Red circles, green triangles and blue squares are used for samples from sites FC, C and L, respectively. The curves at the top and the left of the panels show the distribution of samples on respectively the X and Y axes.

FIGURE 5. Co-inertia analysis between *acdS* and *nifH* diversities (A), *rrs* and *nifH* diversities (B) and *rrs* and *acdS* diversities (C). Projection of the samples (n = 5) is based on both *acdS* (Blue) and *nifH* (Green), *rrs* (Grey) and *nifH* (Green), or *rrs* (Grey) and *acdS* (Blue) diversity variables (level = genus) into a same factorial plan. The vector in black shows the strength of co-trends between the two barycenters of variables as related to each site (L, FC, C). Shorter vectors indicate stronger convergent trends between the two variable groups.

FIGURE S1: Rarefaction curves for *nifH* (A), *acdS* (B) and *rrs* (C) genes**.**

FIGURE S2. RAxML bipartition tree of 3322 sequenced *acdS* alleles from *Poaceae* rhizosphere. The tree was visualized using iTOL software (Letunic I, Bork P. Interactive Tree Of Life (iTOL) v4: recent updates and new developments (2019) *Nucleic Acids Res* doi: 10.1093/nar/gkz239). Branches colored in violet represent the out-group of D-cystein desulfhydrase genes, whereas *acdS* alleles affiliated to *Betaproteobacteria* are shown in khaki, to *Gammaproteobacteria* in blue, to *Actinobacteria* in green, to *Alphaproteobacteria* in red, and to microeukaryotes in orange. The tree can be viewed online at the following link http://itol.embl.de/shared/*acdStree*.

Table 1. Field characteristics of the top (5-30 cm) soil layer.

Field	Soil type	Texture (%)			pH		Organic C	Total N	C/N ratio	Cation exchange (cmol/kg)			
		Sand	Silt	Clay	H_2O	KCl	(g/kg)	(g/kg)		CEC[a]	Ca^{2+}	Mg^{2+}	K^+
FC	Fluvic cambisol	26.9	38.3	34.7	7.1	6.3	31.6	3.4	9.3	22.8	21.2	0.67	0.38
L	Luvisol	42.9	42.9	14.2	7.3	6.7	21.5	1.6	13.4	93.0	10.5	0.33	0.43
C	Calcisol	15.6	74.1	10.3	8.2	7.7	25.9	3.1	8.4	97.0	36.1	0.24	0.29

[a]CEC, cation exchange capacity.

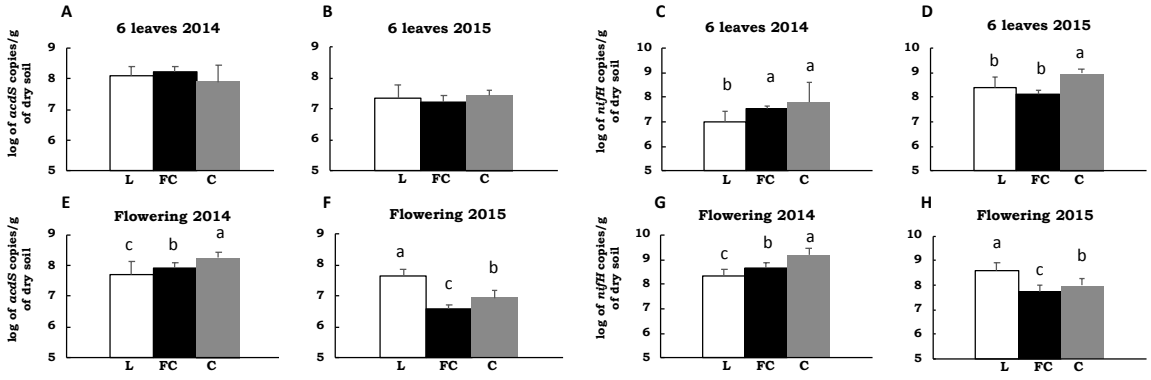

Fig. 1

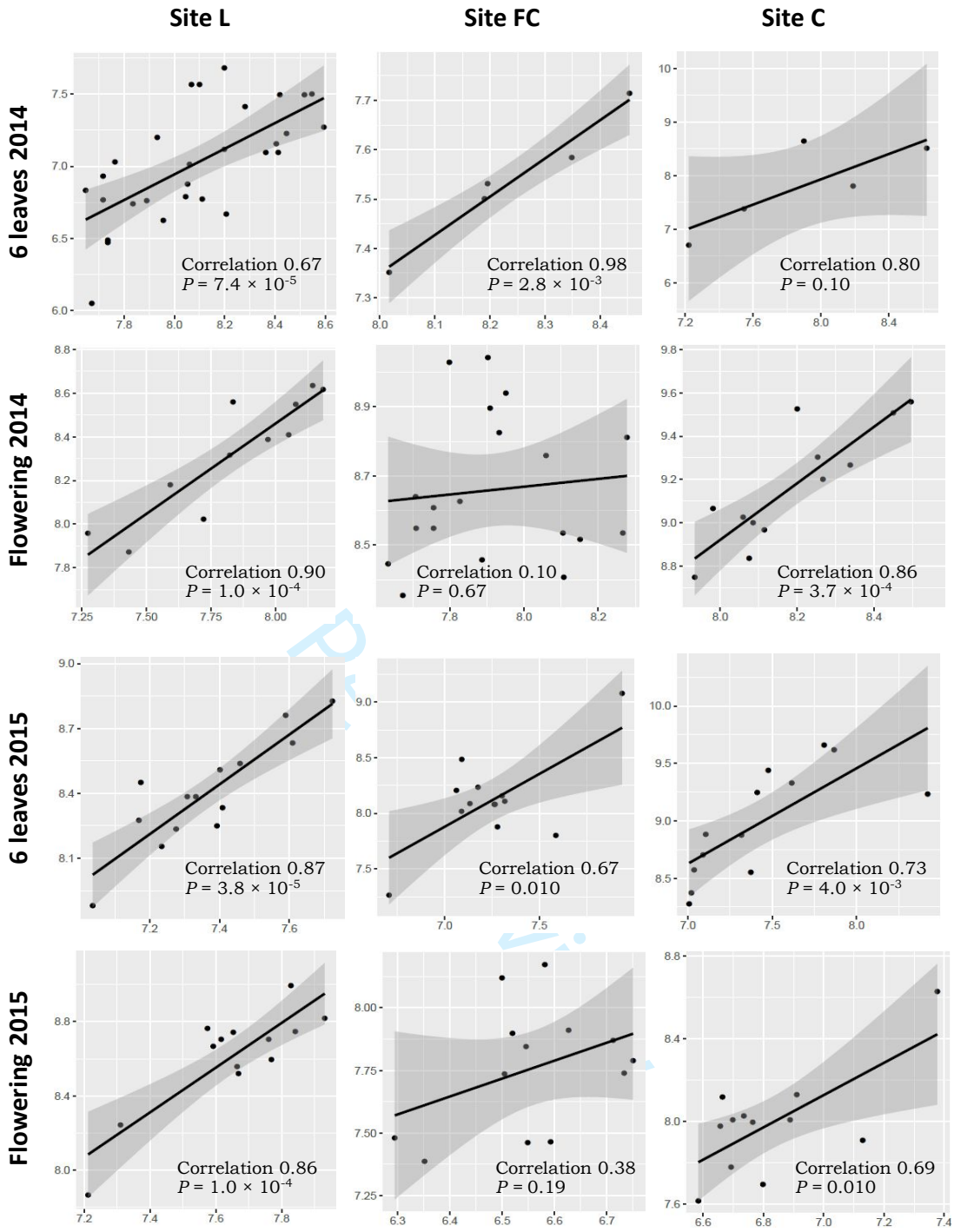

Fig. 2

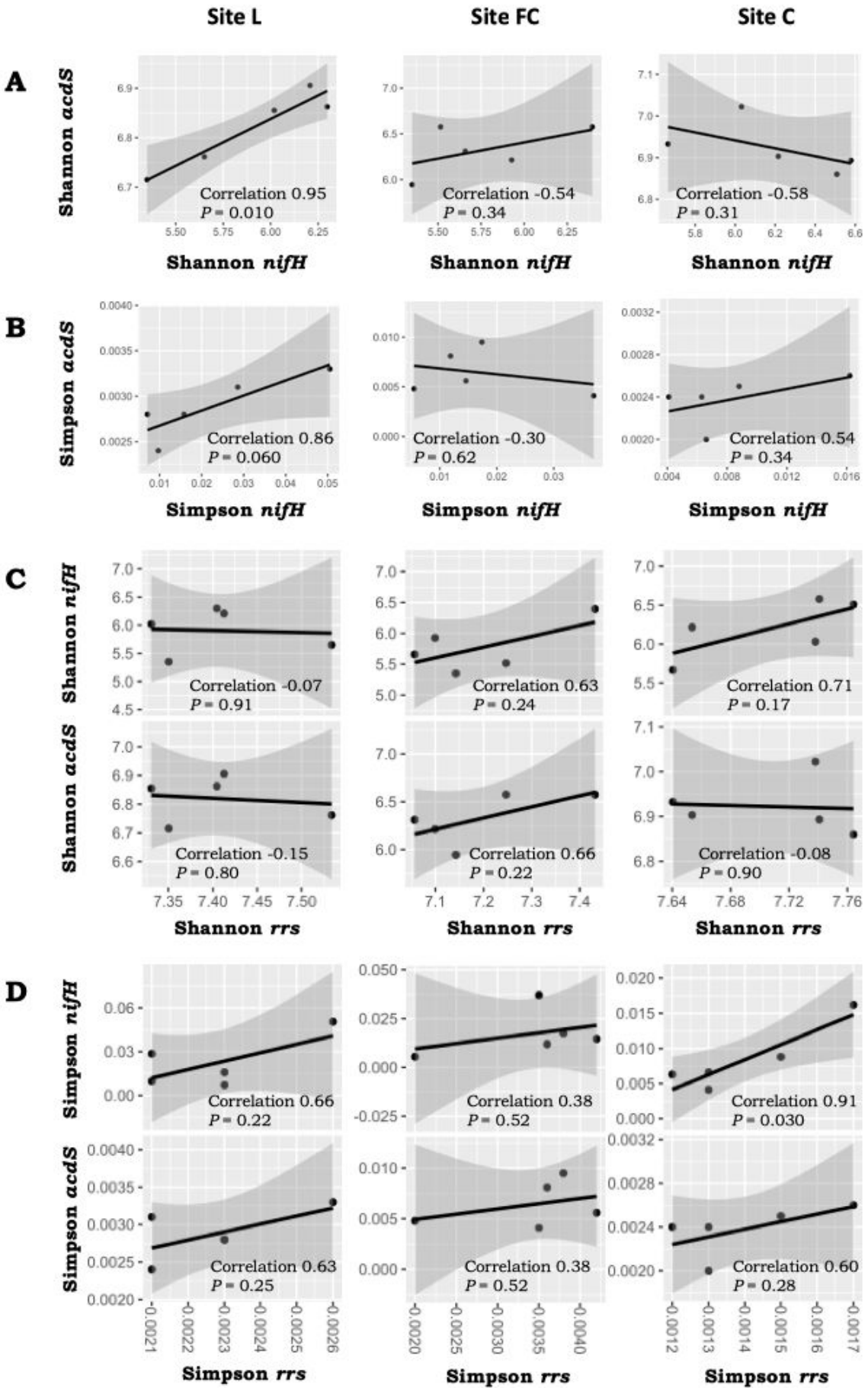
Site L
Site FC
Site C
A
Shannon acdS
Correlation 0.95
P = 0.010
Correlation -0.54
P = 0.34
Correlation -0.58
P = 0.31
Shannon nifH
B
Simpson acdS
Correlation 0.86
P = 0.060
Correlation -0.30
P = 0.62
Correlation 0.54
P = 0.34
Simpson nifH
C
Shannon nifH
Correlation -0.07
P = 0.91
Correlation 0.63
P = 0.24
Correlation 0.71
P = 0.17
Shannon acdS
Correlation -0.15
P = 0.80
Correlation 0.66
P = 0.22
Correlation -0.08
P = 0.90
Shannon rrs
D
Simpson nifH
Correlation 0.66
P = 0.22
Correlation 0.38
P = 0.52
Correlation 0.91
P = 0.030
Simpson acdS
Correlation 0.63
P = 0.25
Correlation 0.38
P = 0.52
Correlation 0.60
P = 0.28
Simpson rrs

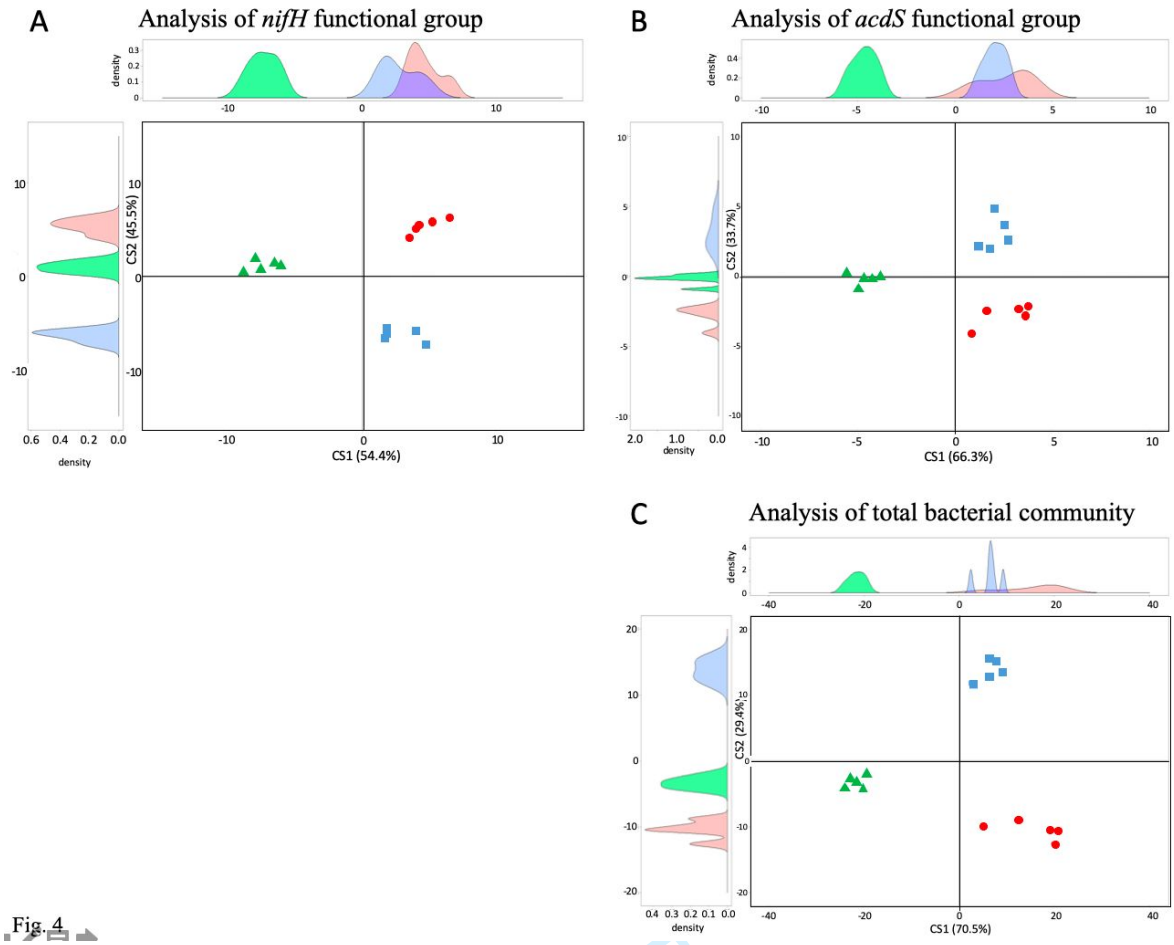

Fig. 4

Figure 5

FIGURE 1. Size of the *acdS* and *nifH* functional groups compared in the three field sites L, FC and C over four sampling times. Means and standard deviations are shown for the *acdS* group at 6 leaves in 2014 (A) and 2015 (B) and at flowering in 2014 (E) and 2015 (F) and for the *nifH* group at 6 leaves in 2014 (C) and 2015 (D) and at flowering in 2014 (G) and 2015 (H). The analysis was done using pooled samples of six roots systems (n= 5) at FC and C and individual root systems (n = 30) at L in 2014, and individual root systems (n = 20) at all three sites in 2015. Statistical differences between sites are indicated by letters a-c (ANOVA and Fischer's LSD tests, $P < 0.05$).

FIGURE 2. Correlation between log numbers of *nifH* (X axis) and *acdS* genes (Y axis). Correlation was established using the Pearson coefficient. The analysis was done using pooled samples of six roots systems (n= 5) at FC and C and individual root systems (n = 30) at L in 2014, and individual root systems (n = 20) at all three sites in 2015.

FIGURE 3. Correlation between Shannon diversity indices of *nifH* and *acdS* (A), Simpson diversity indices of *nifH* and *acdS* (B), Shannon diversity indices of *rrs* and *acdS* or *nifH* (C), and Simpson diversity indices of *rrs* and *acdS* or *nifH* (D). Correlation was established separately at each of the three field sites L, FC and C, using the Pearson coefficient (n = 5).

FIGURE 4. Comparison of *nifH* (A), *acdS* (B) and *rrs* (C) diversity between sites L, FC and C by between-class analysis. Red circles, green triangles and blue squares are used for samples from sites FC, C and L, respectively. The curves at the top and the left of the panels show the distribution of samples on respectively the X and Y axes.

FIGURE 5. Co-inertia analysis between *acdS* and *nifH* diversities (A), *rrs* and *nifH* diversities (B) and *rrs* and *acdS* diversities (C). Projection of the samples (n = 5) is based on both *acdS* (Blue) and *nifH* (Green), *rrs* (Grey) and *nifH* (Green), or *rrs* (Grey) and *acdS* (Blue) diversity variables (level = genus) into a same factorial plan. The vector in black shows the strength of co-trends between the two barycenters of variables as related to each site (L, FC, C). Shorter vectors indicate stronger convergent trends between the two variable groups.

FIGURE S1: Rarefaction curves for *nifH* (A), *acdS* (B) and *rrs* (C) genes**.**

FIGURE S2. RAxML bipartition tree of 3322 sequenced *acdS* alleles from *Poaceae* rhizosphere. The tree was visualized using iTOL software. Branches colored in violet represent the out-group of D-cystein desulfhydrase genes, whereas *acdS* alleles affiliated to *Betaproteobacteria* are shown in khaki, to *Gammaproteobacteria* in blue, to *Actinobacteria* in green, to *Alphaproteobacteria* in red, and to microeukaryotes in orange.

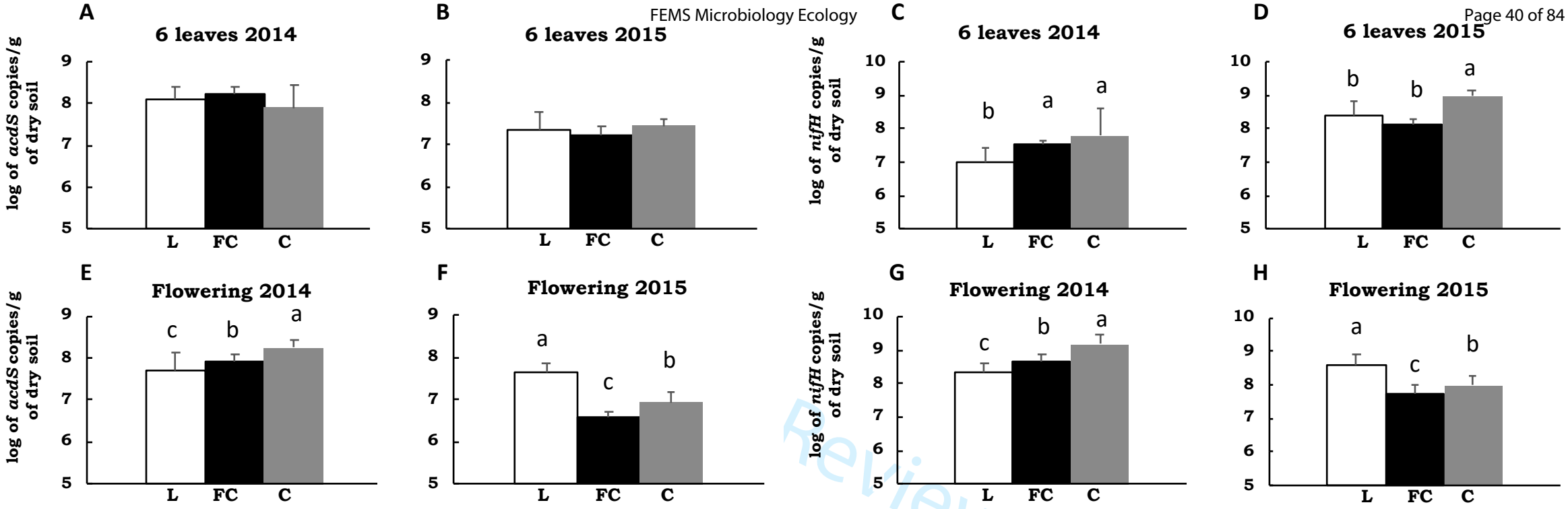
A
6 leaves 2014
log of acdS copies/g of dry soil
B
6 leaves 2015
C
6 leaves 2014
log of nifH copies/g of dry soil
D
6 leaves 2015
E
Flowering 2014
log of acdS copies/g of dry soil
F
Flowering 2015
G
Flowering 2014
log of nifH copies/g of dry soil
H
Flowering 2015
L
FC
C

Fig. 1

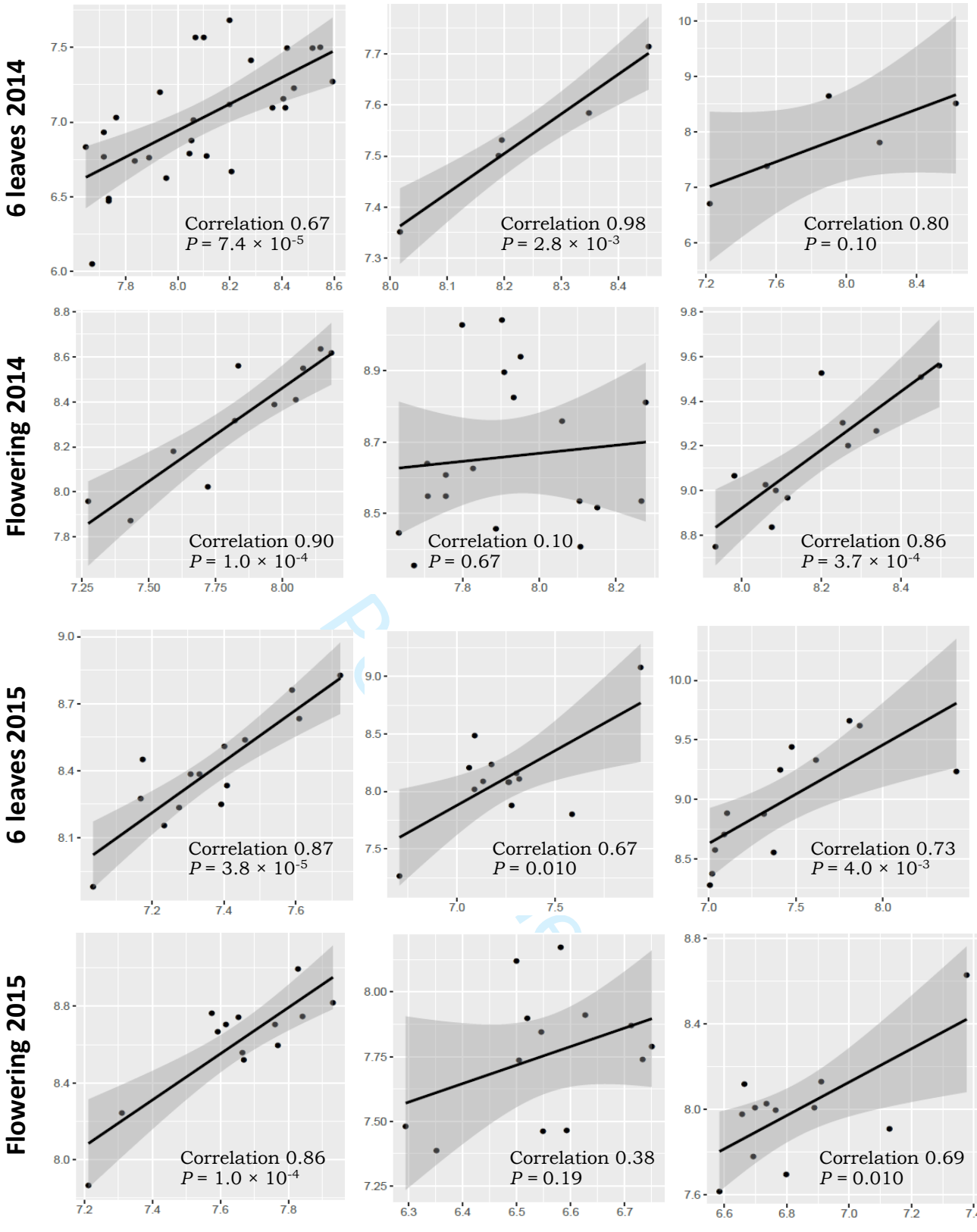
Site L
Site FC
Site C
6 leaves 2014
Flowering 2014
6 leaves 2015
Flowering 2015
Correlation 0.67
P = 7.4 × 10-5
Correlation 0.98
P = 2.8 × 10-3
Correlation 0.80
P = 0.10
Correlation 0.90
P = 1.0 × 10-4
Correlation 0.10
P = 0.67
Correlation 0.86
P = 3.7 × 10-4
Correlation 0.87
P = 3.8 × 10-5
Correlation 0.67
P = 0.010
Correlation 0.73
P = 4.0 × 10-3
Correlation 0.86
P = 1.0 × 10-4
Correlation 0.38
P = 0.19
Correlation 0.69
P = 0.010

Fig. 2

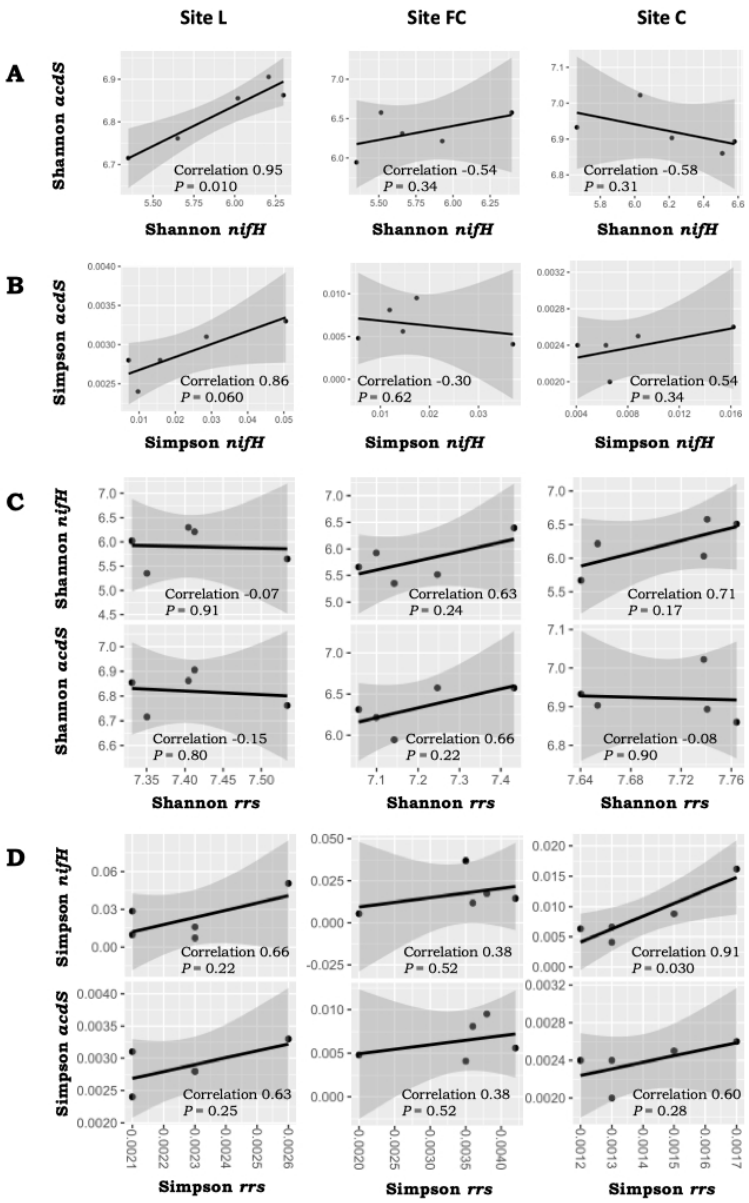

FIGURE 3. Correlation between Shannon diversity indices of nifH and acdS (A), Simpson diversity indices of nifH and acdS (B), Shannon diversity indices of rrs and acdS or nifH (C), and Simpson diversity indices of rrs and acdS or nifH (D). Correlation was established separately at each of the three field sites L, FC and C, using the Pearson coefficient (n = 5).

238x359mm (72 x 72 DPI)

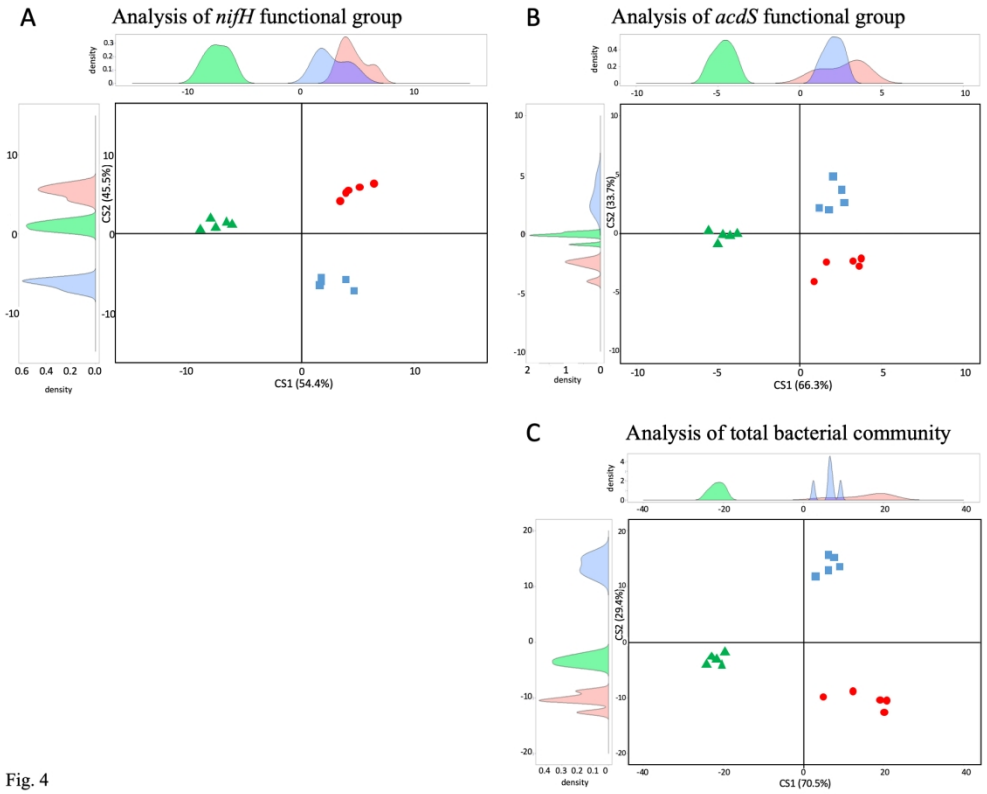

Fig. 4

FIGURE 4. Comparison of nifH (A), acdS (B) and rrs (C) diversity between sites L, FC and C by between-class analysis. Red circles, green triangles and blue squares are used for samples from sites FC, C and L, respectively. The curves at the top and the left of the panels show the distribution of samples on respectively the X and Y axes.

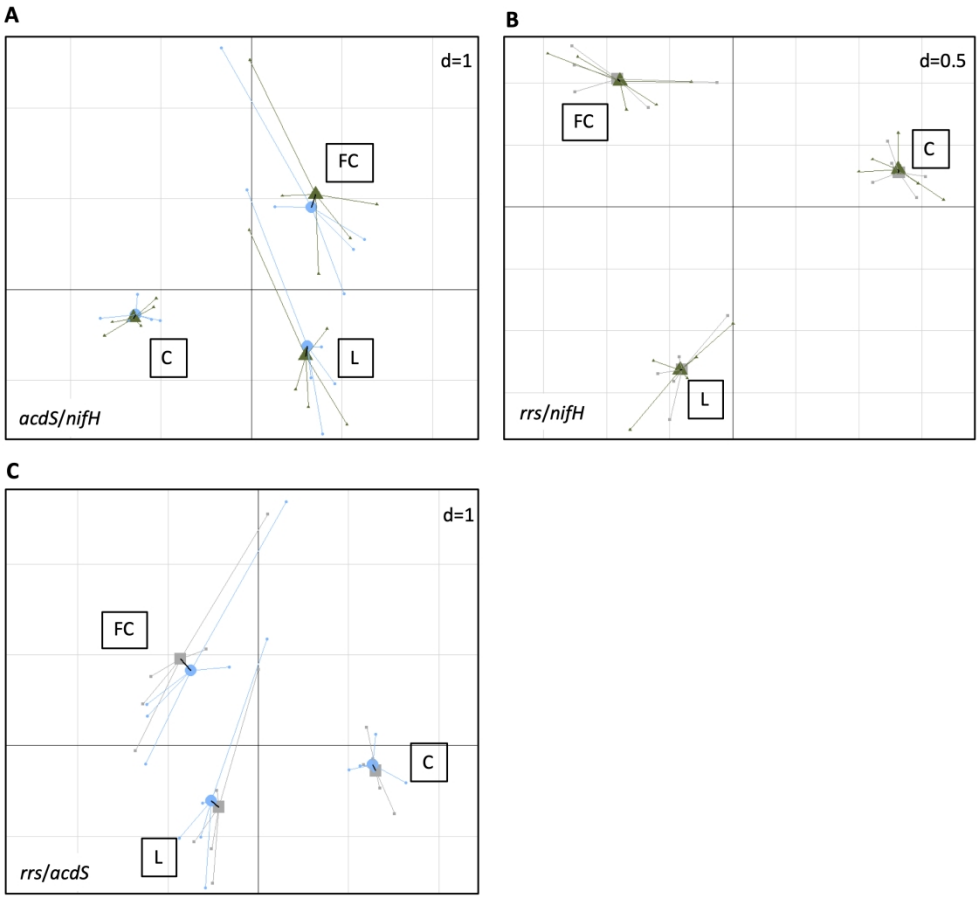

FIGURE 5. Co-inertia analysis between acdS and nifH diversities (A), rrs and nifH diversities (B) and rrs and acdS diversities (C). Projection of the samples (n = 5) is based on both acdS (Blue) and nifH (Green), rrs (Grey) and nifH (Green), or rrs (Grey) and acdS (Blue) diversity variables (level = genus) into a same factorial plan. The vector in black shows the strength of co-trends between the two barycenters of variables as related to each site (L, FC, C). Shorter vectors indicate stronger convergent trends between the two variable groups.

Table 1. Field characteristics of the top (5-30 cm) soil layer.

Field	Soil type	Texture (%)			pH		Organic C	Total N	C/N ratio	Cation exchange (cmol/kg)			
		Sand	Silt	Clay	H_2O	KCl	(g/kg)	(g/kg)		CEC[a]	Ca^{2+}	Mg^{2+}	K^+
FC	Fluvic cambisol	26.9	38.3	34.7	7.1	6.3	31.6	3.4	9.3	22.8	21.2	0.67	0.38
L	Luvisol	42.9	42.9	14.2	7.3	6.7	21.5	1.6	13.4	93.0	10.5	0.33	0.43
C	Calcisol	15.6	74.1	10.3	8.2	7.7	25.9	3.1	8.4	97.0	36.1	0.24	0.29

[a]CEC, cation exchange capacity

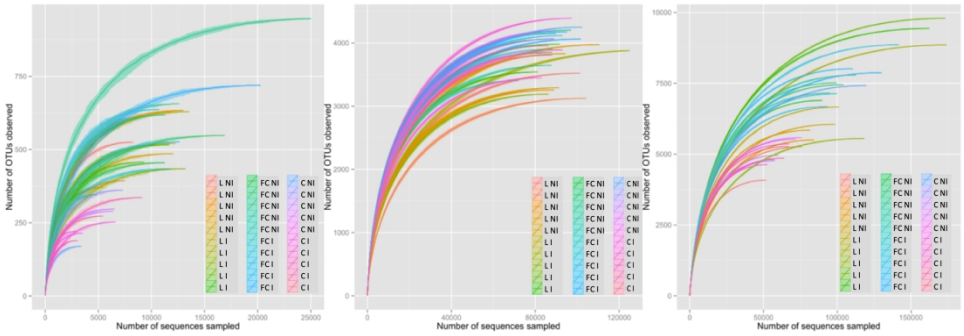

Fig S1

904x322mm (72 x 72 DPI)

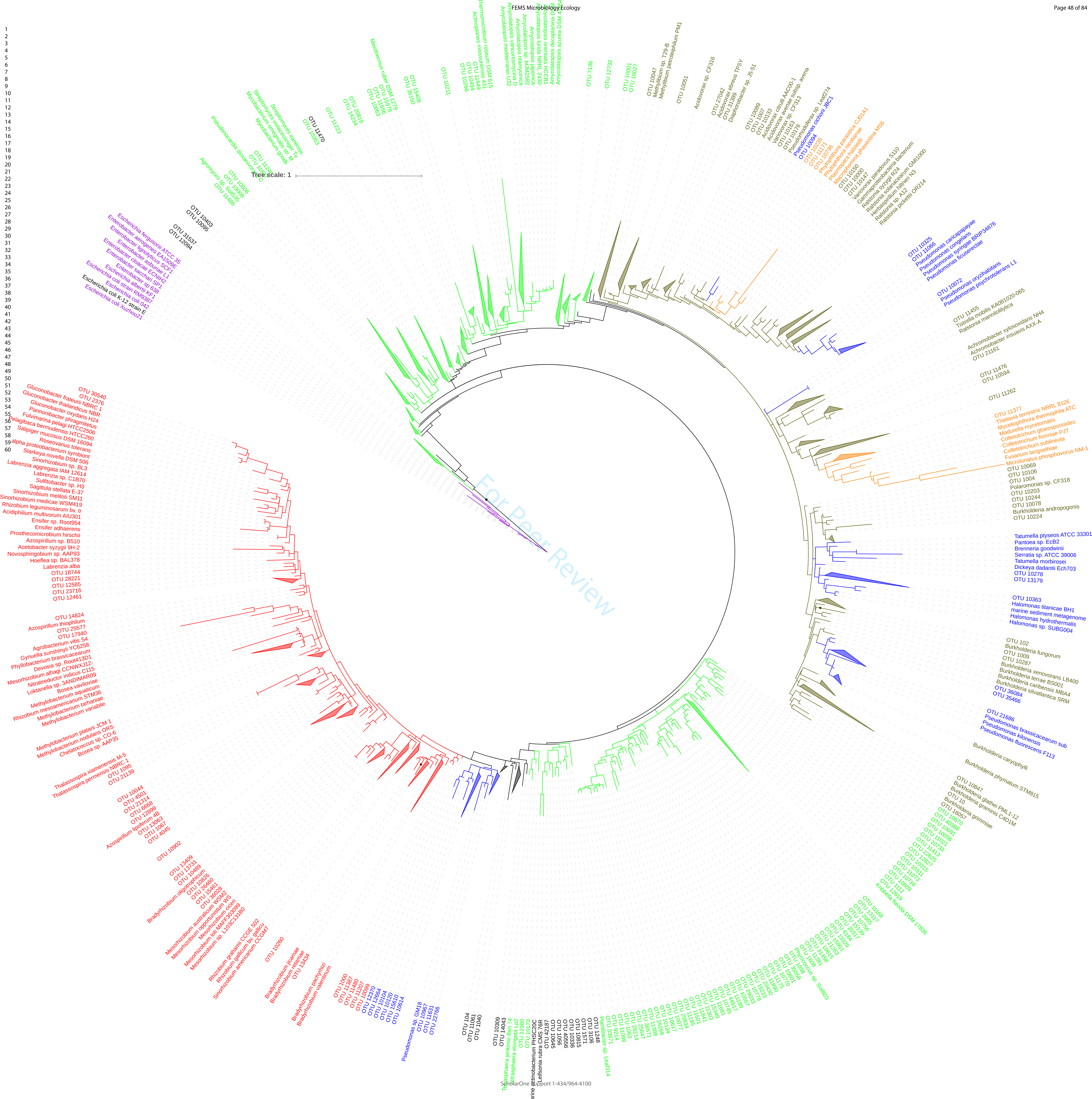

Co-occurrence of rhizobacteria with nitrogen fixation and/or 1-aminocyclopropane-1-carboxylate deamination abilities in the maize rhizosphere

Sébastien Renoud[1‡], Marie-Lara Bouffaud[1‡], Audrey Dubost[1], Claire Prigent-Combaret[1], Laurent Legendre[1,2], Yvan Moënne-Loccoz[1] and Daniel Muller[1*]

[1] Univ Lyon, Université Claude Bernard Lyon 1, CNRS, INRAE, VetAgro Sup, UMR5557 Ecologie Microbienne, 43 bd du 11 novembre 1918, F-69622 Villeurbanne, France

[2] Univ Lyon, Université de St Etienne, F-42000 St Etienne, France

[‡] Current addresses:

S.R. : BGene genetics Bâtiment B Biologie, F-38400 Saint Martin d'Hères, France

M.L.B. : Helmholtz Center for Environmental Research UFZ, Theodor-Lieser-Straβe 4, 06120 Halle, Germany

Running title: *nifH* and *acdS* bacteria on maize

***Corresponding author:** UMR CNRS 5557 Ecologie Microbienne, Université Lyon 1, 43 bd du 11 Novembre 1918, 69622 Villeurbanne cedex, France. Phone: +33 4 72 43 27 14. E-mail: daniel.muller@univ-lyon1.fr

ABSTRACT

The plant microbiota may differ depending on soil type, but these microbiota probably share the same functions necessary for holobiont fitness. Thus, we tested the hypothesis that phytostimulatory microbial functional groups are likely to co-occur in the rhizosphere, using groups corresponding to nitrogen fixation (*nifH*) and 1-aminocyclopropane-1-carboxylate deamination (*acdS*), i.e. two key modes of action in plant-beneficial rhizobacteria. The analysis of three maize fields in two consecutive years showed that quantitative PCR numbers of *nifH* and of *acdS* alleles differed according to field site, but a positive correlation was found overall when comparing *nifH* and *acdS* numbers. Metabarcoding analyses in the second year indicated that the diversity level of *acdS* but not *nifH* rhizobacteria in the rhizosphere differed across fields. Furthermore, between-class analysis showed that the three sites differed from one another based on *nifH* or *acdS* sequence data (or *rrs* data), and the bacterial genera contributing most to field differentiation were not the same for the three bacterial groups. However, co-inertia analysis indicated that the genetic structures of both functional groups and of the whole bacterial community were similar across the three fields. Therefore, results point to co-selection of rhizobacteria harboring nitrogen fixation and/or 1-aminocyclopropane-1-carboxylate deamination abilities.

Keywords: microbiota; phytostimulation; functional group; functional microbiota; holobiont; ITSNTS theory

INTRODUCTION

Plant Growth-Promoting Rhizobacteria (PGPR) colonize plant roots and implement a range of plant-beneficial traits, which may result in enhanced plant development, nutrition, health and/or stress tolerance (Almario et al. 2014; Cormier et al. 2016; Gamalero and Glick 2015; Hartman et al. 2018; Vacheron et al. 2013). As a consequence, PGPR strains have received extensive attention for use as microbial inoculants of crops (Bashan et al. 2014; Couillerot et al. 2013).

Plant-beneficial effects exhibited by PGPR are underpinned by a wide range of modes of actions, which include (i) enhanced nutrient availability via associative nitrogen fixation (Puri et al. 2016, Deynze et al. 2018) or phosphate solubilization (Arruda et al. 2013), (ii) stimulation of root system establishment through phytohormone synthesis (Cassán et al. 2014) or consumption of the ethylene precursor 1-aminocyclopropane-1-carboxylate (ACC) via an enzymatic deamination (Glick 2014), and (iii) the induction of systemic resistance responses in plant (Pieterse and Van Wees 2015). In addition to phytostimulation, certain PGPR may also achieve inhibition of phytoparasites using antimicrobial secondary metabolites (Agaras et al. 2015) or lytic enzymes (Pieterse and Van Wees 2015). Often, PGPR strains display more than one phytostimulatory mode of action, which is considered important for effective plant-beneficial effects (Bashan and de-Bashan 2010; Bruto et al. 2014; Rana et al. 2011; Vacheron et al. 2017). Therefore, the co-occurrence of multiple phytostimulation traits is likely to have been subjected to positive evolutionary selection in PGPR populations to maximize success of the plant-PGPR cooperation. This hypothesis is substantiated by genome sequence analysis of many prominent PGPR strains from contrasted taxa (Bertalan et al. 2009; Chen et al. 2007; Redondo-Nieto et al. 2013; Wisniewski-Dyé et al. 2012).

Even though PGPR strains tend to accumulate several plant-beneficial traits (Bruto et al. 2014), the co-occurrence patterns of these traits are not random. This takes place in part

because many past horizontal gene transfers of the corresponding genes were ancient (Frapolli et al. 2012), often leading to clade-specific profiles of plant-beneficial traits (Bruto et al. 2014). However, the analysis of 304 proteobacterial genomes from contrasted taxa evidenced, overall, the co-occurrence of *nifHDK* (nitrogen fixation) and *acdS* (ACC deamination) based on Exact-Fisher pairwise tests (Bruto et al. 2014), raising the possibility that nitrogen fixation and ACC deamination might be useful traits when combined in a bacterium. Indeed, nitrogen fixation and ACC deamination occur together in various rhizobacteria (Blaha et al. 2006; Duan et al. 2009; Jha et al. 2012; Ma, Guinel, and Glick, 2003; Nukui et al. 2006), but the relation between both traits can be complex. In *Azospirillum lipoferum* 4B for instance, the plasmid-borne gene *acdS* is eliminated during phase variation while *nif* genes are maintained (Prigent-Combaret et al. 2008), and in *Mesorhizobium loti* transcription of *acdS* is controlled by the nitrogen fixation regulator gene *nifA2* (Nukui et al. 2006). Moreover, ACC deamination was described as facilitator of the legume-rhizobia symbiosis (Ma et al. 2003; Nascimento et al. 2012).

At the scale of an individual plant, the rhizosphere is colonized by a diversified range of bacteria, including *nifH acdS* bacteria as well as bacteria harboring only *nifH* or *acdS* (Blaha et al. 2006; Bouffaud et al. 2018). There is additional level of complexity in that many of these bacteria are PGPR, but some of them are not (Bruto et al. 2014). However, the overall impact of nitrogen fixation and ACC deamination on the plant is likely to be the sum of the contribution of individual root-colonizing bacteria displaying these traits. This raises the question whether there is, for the plant, an optimal balance between the functional microbial groups of *nifH* rhizobacteria and *acdS* rhizobacteria in the rhizosphere. On this basis, we tested here the hypothesis that rhizobacteria with either nitrogen fixation ability or ACC deamination ability (or with both) co-occur on roots. For that purpose, we used three maize fields under reduced nitrogen fertilization practices, with samplings carried out at 6-leaf and flowering stages during two consecutive years, and numbers of *nifH* and *acdS* rhizobacteria were monitored by

quantitative PCR. In addition, *nifH* and *acdS* rhizobacteria were assessed by metabarcoding (MiSeq Illumina sequencing) of *nifH* and *acdS* genes at one sampling, in parallel to sequencing of 16S rRNA genes for the whole rhizobacterial community.

2. MATERIALS AND METHODS

2.1. Field experiment

The experiment was conducted in 2014 and 2015 at field sites located in Chatonnay (L), Sérézin-de-la-Tour (FC) and Saint Savin (C), near the town of Bourgoin-Jallieu (Isère, France). According to the FAO soil reference base, L field corresponds to a luvisol, FC a fluvic cambisol and C a calcisol (Table 1). The trial set-up has been described in Rozier et al. (2017).

For each of the fields, the crop rotation consists in one year wheat, six years maize and one year rapeseed, and wheat was grown the year before the 2014 experiment. The maize sowing season ranges from middle April to middle May in the area. Maize seeds (*Zea mays* 'Seiddi'; Dauphinoise Company, France) were sown on April 18 (FC) and 23 (C and L) in 2014 and April 30 (C) and May 11 (FC and L) in 2015. Five replicate plots, which were 12 (FC and C) or 8 (L) maize rows wide and 12 m long, were defined in each field. The fields were undergoing a reduction in chemical fertilization usage and did not receive any nitrogen fertilizers in 2014 and 2015. Only non-inoculated plots from the overall trial (Rozier et al. 2017) were used.

2.2. Plant sampling

In 2014 and 2015, plants were sampled at six leaves and at flowering. In 2014, the first sampling was done on May 25 (FC) and 26 (C and L). On each replicate plot, six plants were chosen randomly, the entire root system was dug up and shaken vigorously to dislodge soil loosely

adhering to the roots. At sites FC and C, one pooled sample of six roots system was obtained per plot, i.e. a total of five pooled samples per field site. At site L, each of the six roots system was treated individually to obtain 30 samples. The second sampling was done on July 8 (FC and C) and 9 (L), on all five plots. Six plants were sampled per plot and treated individually to obtain 30 samples per field site.

In 2015, the first sampling was done on May 27 (C), June 5 (FC) and June 8 (L). In each replicate plot, four root systems were sampled and treated individually to obtain 20 samples per field site. The second sampling was done on July 15 (C), 16 (FC) and 17 (L), and four root systems were sampled and treated individually to obtain 20 samples per field site.

Each sample was immediately flash-frozen on site, in liquid nitrogen, and lyophilized back at the laboratory (at -50°C for 24 h). Roots and their adhering soil were separated and the latter stored at -80°C.

2.3. DNA extraction from root-adhering soil

DNA from root-adhering soil was extracted with the FastDNA SPIN kit (BIO 101 Inc., Carlsbad, CA). To this end, 500 mg (for the pooled samples from FC and C in 2014) or 300 mg samples (for all other samples) were transferred in Lysing Matrix E tubes from the kit, and 5 µl of the internal standard APA9 (10^9 copies ml^{-1}) was added to each Lysing Matrix E tube to normalize DNA extraction efficiencies between rhizosphere samples, as described (Park and Crowley, 2005; Couillerot et al. 2010). This internal standard APA9 (i.e. vector pUC19 with cassava virus insert; GenBank accession number AJ427910) requires primers AV1f (CACCATGTCGAAGCGACCAGGAGATATCATC) and AV1r (TTTCGATTTGTGACGTGGACAGTGGGGGC). After 1 h incubation at 4°C, DNA was extracted and eluted in 50 µl of sterile ultra-pure water, according to the manufacturer's instructions. DNA concentrations were assessed by Picogreen (ThermoFisher).

2.4. Size of microbial functional groups

The amounts of *nifH* genes were estimated by quantitative PCR based on the primers polF/polR (Poly, Jocteur Monrozier, and Bally, 2001), as described by Bouffaud et al. (2016). The reaction was carried out in 20 µl containing 4 µl of PCR-grade water, 1 µl of each primer (final concentration 0.50 µM), 10 µl of LightCycler-DNA Master SYBR Green I master mix (Roche Applied Science, Meylan, France) and 2 µl of sample DNA (10 µg). The cycling program included 10 min incubation at 95°C, followed by 50 cycles of 95°C for 15 s, 64°C for 15 s and 72°C for 10 s. Melting curve calculation and Tm determination were performed using the Tm Calling Analysis module of Light-Cycler Software v.1.5 (Roche Applied Science).

The amount of *acdS* genes was estimated by quantitative PCR based on the primers acdSF5/acdSR8 (Bouffaud et al. 2018). The reaction was carried out in 20 µl containing 4 µl of PCR grade water, 1 µl of each primer (final concentration 1 µM), 10 µl of LightCycler-DNA Master SYBR Green I master mix (Roche Applied Science) and 2 µl of sample DNA (10 µg). The cycling program included 10 min incubation at 95°C, followed by 50 cycles of 94°C for 15 s, 67°C for 15 s and 72°C for 10 s. The fusion program for melting curve analysis is described above.

Real-time PCR quantification data were converted to gene copy number per gram of lyophilized root-adhering soil, as described (Bouffaud et al. 2018; Bouffaud et al. 2016).

2.5. *nifH*, *acdS* and *rrs* sequencing from rhizosphere DNA

Sequencing was performed on 2015' samples taken when maize reached 6 leaves. Each sample was an equimolar composite sample of four DNA extracts obtained from root-adherent soil, resulting in 5 samples per field site, i.e. a total of 15 samples. DNA extracts were sent to MR DNA laboratory (www.mrdnalab.com; Shallowater, TX) for sequencing.

For *nifH* and *acdS* sequencing, PCR primers were the same ones used for quantitative PCR (i.e., polF/polR for *nifH* and acdSF5/acdSR8 for *acdS*). For *rrs* sequencing, PCR primers 515/806 were chosen for the V4 variable region of the 16S rRNA gene. For all three genes, the forward primer carried a barcode. Primers were used in a 30-cycle PCR (5 cycles implemented on PCR products), using the HotStarTaq Plus Master Mix Kit (Qiagen, Valencia, CA) under the following conditions: 94°C for 3 min, followed by 28 cycles of 94°C for 30 s, 53°C for 40 s and 72°C for 1 min, with a final elongation step at 72°C for 5 min. PCR products were checked in 2% agarose gel to determine amplification success and relative band intensity. Multiple samples were pooled together in equal proportions based on their molecular weight and DNA concentrations. Pooled samples were purified using calibrated Ampure XP beads and used to prepare a DNA library following Illumina TruSeq DNA library preparation protocol. Sequencing was performed on a MiSeq following the manufacturer's guidelines.

Sequence data were processed using the analysis pipeline of MR DNA. Briefly, sequences were depleted of barcodes, sequences < 150 bp or with ambiguous base calls removed, the remaining sequences denoised, operational taxonomic units (OTUs; defined at 3% divergence threshold for the three genes) generated, and chimeras removed. Final OTUs were taxonomically classified using BLASTn against a curated database derived from Greengenes (DeSantis et al. 2006), RDPII (http://rdp.cme.msu.edu) and NCBI (www.ncbi.nlm.nih.gov). Final OTUs of the *acdS* sequencing were classified using an in-house curated *acdS* database, obtained after curation of *acdS* homolog genes from the FunGene *acdS* 8.3 database, as described by Bouffaud et al. (2018). Diversity indices of Shannon (H) and Simpson (1-D) were calculated using sequencing subsample data for which each sample had the same number of sequences.

An *acdS* phylogenetic tree (based on maximum-likelihood method) was computed using *acdS* sequences from ten arbitrarily-chosen OTUs per genus recovered in our sequencing data

and from one reference taxa for each genus, and related D-cystein desulfhydrase genes D-cystein desulfhydrase genes from strains *Escherichia coli* strains K-12, ER3413, 042 and RM9387, *Escherichia albertii* KF1, *Escherichia fergusonii* ATCC 35469, *Enterobacter sacchari* SP1, *Enterobacter cloacae* ECNIH2, *Enterobacter asburiae* L1, *Enterobacter* sp. 638 and *Enterobacter lignolyticus* SCF1 (used as out-group).

2.6. Statistical analysis

Statistical analysis of quantitative PCR data was carried out by ANOVA and Fishers' LSD tests. For each gene sequenced, comparison of bacterial diversity between field sites was carried out by Between-Class Analysis (BCA) using ADE4 (Chessel et al. 2004; Culhane et al. 2005; Dray, Dufour, and Chessel, 2007) and ggplot2 packages for R, and the 12 genera contributing most to field site differentiation were identified. To assess co-trends between *nifH* and *acdS* variables, as well as between *rrs* and *nifH* or *acdS* variables, sequence data were also assessed using co-inertia analysis (CIA) (Dray et al. 2003; Dray et al. 2007), which was computed with the ADE4 package in the R statistical software environment (Culhane et al. 2005). CIA is a dimensional reduction procedure designed to measure the similarity of two sets of variables, here the proportions of *nifH* and *acdS* bacterial genera obtained during between-class analyses. Its significance was assessed using Monte-Carlo tests with 10,000 permutations. Unless otherwise stated, statistical analyses were performed using R v3.1.3 (Team, 2014), at $P < 0.05$ level.

2.7. Nucleotide sequence accession numbers

Illumina MiSeq paired-end reads have been deposited in the European Bioinformatics Institute (EBI) database under accession numbers PRJEB14347 (ERP015984) for *rrs*; PRJEB14346 (ERP015983) for *nifH*, PRJEB14343 (ERP015981) for *acdS.*

3. RESULTS

3.1. Relation between numbers of *nifH* and *acdS* alleles in the three field sites

The number of *acdS* bacteria in the rhizosphere of maize harvested at 6-leaf stage in 2014 (7.87 to 17.4 × 10^7 *acdS* gene copies g^{-1} of dry soil) and 2015 (1.76 to 2.81 × 10^7 *acdS* gene copies g^{-1} of dry soil) did not differ significantly between field sites (Figure 1AB). At flowering stage, however, the number of *acdS* bacteria differed from one site to the next, both in 2014 and in 2015 (Figure 1EF). At that growth stage, the lowest rhizosphere abundance was observed in site L (5.08 × 10^7 *acdS* gene copies g^{-1} of dry soil) and the highest in site C (1.76 × 10^8 *acdS* gene copies g^{-1} of dry soil) in 2014, whereas site ranking was the opposite in 2015 (8.35 versus 44.0 × 10^6 *acdS* gene copies g^{-1} of dry soil for sites C and L, respectively).

The numbers of *nifH* rhizobacteria differed according to field site (Figure 1CDGH). In 2014, the lowest *nifH* abundance was observed in rhizospheres of site L (1.06 and 20.8 × 10^7 *nifH* gene copies g^{-1} of dry soil at respectively six leaves and flowering) and the highest in those of site C (6.43 and 147.0 × 10^7 *nifH* gene copies g^{-1} of dry soil at respectively six leaves and flowering) (Figure 1CG). In 2015, the numbers of *nifH* rhizobacteria was higher in site C (9.31 × 10^8 *nifH* gene copies g^{-1} of dry soil) than in FC (1.30 × 10^8 *nifH* gene copies g^{-1} of dry soil) and L (2.52 × 10^8 *nifH* gene copies g^{-1} of dry soil) at six leaves, whereas the situation was opposite at flowering, with higher abundance in site L (40.7 × 10^7 *nifH* gene copies g^{-1} of dry soil) than C (9.81 × 10^7 *nifH* gene copies g^{-1} of dry soil) and FC (5.66 × 10^7 *nifH* gene copies g^{-1} of dry soil) (Figure 1DH).

When comparing the log numbers of *nifH* rhizobacteria and *acdS* rhizobacteria across the 12 site × sampling combinations, significant ($3.8 \times 10^{-5} < P < 0.01$) positive correlations ($0.67 < r < 0.98$, $n = 20$) were found in 9 of 12 cases, with only three correlations that were not

significant, i.e. in site C at 6-leaf stage in 2014 (P = 0.10, n = 5) and FC at flowering in 2014 (P = 0.67, n = 5) and 2015 (P = 0.19, n = 20) (Figure 2). In summary, moderate but significant differences in the numbers of *nifH* and/or *acdS* rhizobacteria could take place according to field site, sampling year and/or maize phenology, and in most cases a positive correlation was found between the log values of both numbers.

3.2. Relation between diversities of *nifH* and *acdS* alleles in the three field sites

Illumina MiSeq sequencing of *nifH* and *acdS* (as well as *rrs*) was carried out on 15 rhizosphere samples from 6-leaf maize grown in 2015. For *nifH*, 1,342,966 reads were obtained (10,775 to 62,752 sequences per sample), for a total of 36,241 OTUs. Rarefaction analysis showed that curves reached a plateau (Figure S1A). Subsampling was done with 10,775 sequences per sample, for a total of 34,459 OTUs. For *acdS*, 5,490,230 reads were obtained (68,376 to 139,245 sequences per sample), with a total of 32,468 OTUs. Rarefaction curves reached a plateau (Figure S1B). Subsampling was done with 68,376 sequences per sample, for a total of 26,246 OTUs. After quality filtering, 6,082,255 reads were obtained for *rrs* (51,696 to 223,926 sequences per sample), giving a total of 39,600 OTUs (3% cut-off). Rarefaction analysis showed that the sequencing effort captured most of the diversity with curves reaching a plateau (Figure S1C). Subsampling was done with 51,696 sequences per sample, for a total of 25,437 OTUs.

The effect of field site on *nifH* diversity of diazotrophic bacteria was not significant based on analysis of Shannon and Simpson indices. Conversely, the effect of field site on *acdS* diversity of ACC deaminase bacteria was significant based on the Shannon ($P = 1.9. \times 10^{-4}$) and Simpson indices ($P = 8.6 \times 10^{-4}$). The Shannon index was lower in FC (6.32) than in L (6.82) and C (6.92), whereas the Simpson index was higher in FC (6.42×10^{-3}) than in L (2.88×10^{-3}) and C (2.38×10^{-3}). The effect of field site on *rrs* diversity of the total bacterial

community was significant based on the Shannon ($P = 1.8 \times 10^{-5}$) and Simpson indices ($P = 1.6 \times 10^{-4}$). As in the case of *acdS* data, the Shannon index was lower in FC (7.20) than in L (7.41) and C (7.71), whereas the Simpson index was higher in FC (3.42×10^{-3}) than in L (2.28×10^{-3}) and C (1.40×10^{-3}).

The correlation (n = 5) between *nifH* diversity and *acdS* diversity was positive and significant at site L, when considering both the Shannon index (r = 0.98 ; $P = 0.01$; Figure 3) and the Simpson index (r = 0.86 ; $P = 0.06$; Figure 3). However, the correlation was not significant at the other two sites, regardless of the diversity index. When considering also *rrs* diversity, a significant correlation was found only with *nifH* diversity at site C (r = 0.91 ; $P = 0.03$; Figure 3). In summary, there was no relation between the diversities of *nifH* rhizobacteria and *acdS* rhizobacteria, based on comparison of diversity indices in the three field sites and correlation analyses at two of the three field sites.

3.3. Relation between prevalence of *nifH* and/or *acdS* rhizobacterial taxa in the three field sites

Between-class analysis of *nifH* data showed that the composition of diazotrophic bacteria differed according to field site (Figure 4A). The first axis (54% of between-class variability) distinguished site C from FC and L, and the 12 genera contributing most to this differentiation were *Xanthobacter, Dechloromonas, Methyloferula, Ideonella, Nitrospirillum* and *Tolumonas* (more prevalent in C than in L and FC), as well as *Desulfovibrio, Selenomonas, Ruminiclostridium, Paludibacter, Gloeocapsopsis* and *Ruminococcus* (less prevalent in C than in FC and L). The second axis (46% of between-class variability) distinguished site L from the two other sites, and the 12 genera contributing most to this differentiation included *Rhizobium, Gluconacetobacter, Skermanella, Leptothrix, Streptomyces* and *Methylocapsa* (more prevalent in L than in FC and C), as well as *Marichromatium, Pelobacter, Gordonibacter, Desulfobulbus, Desulfovibrio* and *Sideroxydan* (less prevalent in L than in C and FC).

Between-class analysis of *acdS* data showed that the composition of ACC deaminase bacteria differed according to field site (Figure 4B). The first axis (66% of between-class variability) distinguished site C from FC and L, and the 12 genera contributing most to this differentiation were *Achromobacter, Azospirillum, Pseudolabrys, Roseovarius,* one unassigned OTU and *Polaromonas* (more prevalent in C than in L and FC), as well as *Cupriavidus, Burkholderia, Bosea, Bradyrhizobium* and *Methylobacterium* (less prevalent in C than in FC and L). The second axis (34% of between-class variability) distinguished each of the three sites from one another, and the 12 genera contributing most to this differentiation included *Azorhizobium, Pseudomonas, Gluconobacter, Collimonas, Herbaspirillum* and *Burkholderia* (more prevalent in FC than in C and L), as well as *Ralstonia, Loktanella, Devosia, Variovorax, Novosphingobium* and *Chelatococcus* (more prevalent in L than in C and FC).

Between-class analysis of *rrs* data showed that the composition of the total bacterial community differed according to field site (Figure 4C). The first axis (71% of between-class variability) distinguished C from the two other sites, and the 12 genera contributing most to this differentiation were *Algisphaera, Fibrobacter, Amaricoccus, Hirschia, Desulfacinum* and *Saccharophagus* (more prevalent in C than in L and FC), as well as *Actinomadura, Lutispora, Bacillus, Rhodopseudomonas, Kouleothrix* and *Roseiflexus* (less prevalent in C than in FC and L). The second axis (29% of between-class variability) distinguished site L from FC and C, and the 12 genera contributing most to this differentiation included *Flavobacterium, Gluconobacter, Maricaulis, Prolixibacter, 'Candidatus* Xiphinematobacter', *Chthoniobacter* (more prevalent in FC than L), as well as *Conexibacter, Hyphomicrobium, Pseudonocardia, Tumebacillus, Chelatococcus* and *Mycobacterium* (less prevalent in FC than in L).

In summary, between-class analysis of *nifH* and *acdS* data indicated that the composition of diazotrophic bacteria and of ACC deaminase bacteria differed according to field site, but the main discriminant genera differed completely for both types of bacteria. In both cases, the discriminant taxa were also different from the main range of bacterial taxa distinguishing the three sites most when comparing the latter based on *rrs* data, at the scale of the entire rhizobacterial community.

3.4. Relation between the genetic structures of *nifH* and *acdS* rhizobacteria in the three field sites

Since there was a positive correlation between log numbers of *nifH* and/or *acdS* rhizobacteria but the corresponding bacterial genera discriminating most between the three fields studied were not the same, the co-structuration between *nifH* and *acdS* diversity was explored by co-inertia analysis to compare more globally the genetic structures of these rhizobacterial groups across the three field sites. Monte-Carlo permutation tests showed a significant co-structuration

($P = 9 \times 10^{-5}$) of *nifH* and *acdS* rhizobacteria, with a RV coefficient of 0.83. This accounted for 57% of data variability. The plot of the co-inertia matrix illustrates the strength of the relationship between *acdS* and *nifH* diversities, as superposition of *acdS* and *nifH* groups showed a strong co-trend in all three field sites (Figure 5).

Co-inertia analyses of *nifH* and *acdS* diversities were also performed with *rrs* diversity, and permutations tests also showed co-structuration in both cases, with respectively RV coefficients of 0.89 and 0.91, the two axes explaining 52% and 69% of variability. Superposition of *rrs* community with *acdS* and with *nifH* groups indicated a strong co-trend across the three fields.

In summary, the genetic structures of *nifH* and *acdS* rhizobacterial groups across the three field sites were very close. Co-inertia was strong also when comparing each with the whole rhizobacterial community based on *rrs* data.

4. DISCUSSION

The current work made use of molecular tools available to characterize functional groups of *nifH* and *acdS* bacteria. Quantification of *nifH* rhizobacteria was performed with primers PolF/PolR (Poly et al. 2001) rather than other well-established primers such as Zf/Zr (Zehr and McReynolds, 1989) since the latter are not effective for quantitative PCR (Boyd and Peters 2013; Gaby and Buckley 2017; Poly et al. 2001). The same primers have also been used for sequencing, both for consistency and efficacy for diazotroph characterization (Mårtensson et al. 2009; Wartiainen et al. 2008). Recently, *acdS* primers suitable for monitoring of ACC deamination bacteria have been made available (Bouffaud et al. 2018). These primers are effective to amplify true *acdS* genes while not amplifying related D-cystein desulfhydrase genes coding for other PLP-dependent enzymes, which was verified again in the current work (Figure

S2). Indeed, phylogenetic analysis of the *acdS* sequences showed that none clustered within the out-group (built with strains harboring D-cystein desulfhydrase genes), confirming that the sequences obtained were true *acdS* sequences, as highlighted in previous studies (Blaha et al. 2006; Bouffaud et al. 2018; Li et al. 2015; Nascimento et al. 2012).

The level of taxonomic information carried by *nifH* sequences has been described in the literature, showing that *nifH* was sufficiently conserved to enable reliable taxonomic affiliations including for the assessment of rhizobacteria (Vinuesa et al. 2005), and its phylogeny was congruent with the one derived from *rrs* (Achouak et al. 1999; Zehr et al. 2003). As for *acdS*, phylogenetic analysis of the new sequences obtained (along with reference *acdS* sequences) confirmed that the taxonomic affiliations made at the genus level were correct. However, the 130-bp *acdS* amplicons obtained with the current quantitative PCR primers do not enable any taxonomic affiliation below the genus level, i.e. at the species level (Bouffaud et al. 2018).

In this work, the hypothesis that *nifH* and *acdS* rhizobacterial populations co-occur on roots was assessed with maize taken from three fields, using quantitative PCR and MiSeq sequencing. The results that were obtained did substantiate this hypothesis, based on (i) positive correlations between the sizes of *nifH* and *acdS* rhizobacterial groups, and (ii) comparable genetic structures indicated by inertia analysis for both functional groups across the three field sites studied. Several studies have assessed the co-occurrence of particular microorganisms and measured between-taxa correlations in soil systems (Barberán et al. 2011; Freilich et al. 2010), but few have done so at the level of functional groups. For instance, co-occurrence analysis of nitrite-dependent anaerobic ammonium oxidizers and methane oxidizers in paddy soil showed that the structure of these communities changed with soil depth (Wang et al. 2012). The co-occurrence of plant-beneficial functions in the rhizosphere has been investigated, but often the assessment was restrained to narrow taxonomic levels, such as within the *Pseudomonas* genus (Almario et al. 2014; Frapolli et al. 2012; Vacheron et al. 2016). It is interesting to note that not

all microorganisms harboring *acdS* and/or *nifH* expressed the corresponding functions in rhizosphere based on assessment of qRT-PCR data, as previously described for *nifH* (Bouffaud et al. 2016) or *acdS* (Bouffaud et al. 2018).

Specific taxa can be selected by environmental conditions prevailing on plant roots (Bakker et al. 2014; Berg and Smalla, 2009; Raaijmakers et al. 2009; Vandenkoornhuyse et al. 2015). Thus, a first possibility to account for the co-occurrence of both functional groups could be that both *nifH* bacteria and *acdS* bacteria do well in the maize rhizosphere. Indeed, both types of bacteria are readily found on roots (Almario et al. 2014; Arruda et al. 2013; Blaha et al. 2006; Bruto et al. 2014; Bruto et al. 2014; Mårtensson et al. 2009). Such co-occurrence would make sense in ecological terms, because associative nitrogen fixation and ACC deamination are functions limiting plant nutrient deficiency by supplying nitrogen (Pii et al. 2015) and enhancing root system development (thereby improving uptake of mineral nutriments including nitrogen) (Glick, 2014), respectively.

A second possibility could be that bacteria that harbor both genes/functions are well adapted to maize roots. Indeed, Bruto et al. (2014) showed that the *nif* operon co-occurred with *acdS* in several bacterial clades, and for instance the genera *Bradyrhizobium* or *Burkholderia* contain several species harboring both functions (Bruto et al. 2014). Furthermore, the co-inertia between these two functional groups and the total community raises the possibility that additional functions could also be present in addition to associative nitrogen fixation and ACC deamination. Indeed, comparative genomics studies showed that bacterial taxa display multiple specific functions, including plant interaction functions (Bruto et al. 2014; Lassalle et al. 2015; Vacheron et al. 2017), and thus these functions would also be co-selected when selecting the corresponding *rrs*-based taxa. In the current study, *Bradyrhizobium* represented 17 to 25% of *acdS*$^+$ bacteria and 20 to 42% of *nifH*$^+$ bacteria in the maize rhizosphere, and the high proportion of this bacterial clade may contribute to the co-occurence of diazotrophs and ACC deaminase

producers that was found. However, when the 10,369 completely-sequenced bacterial genomes available in the NCBI database were screened, it showed that 833 of them harbored *acdS* and 461 others *nifH*, but only 122 genomes had both genes. Therefore, it could be that this second possibility is insufficient for a complete explanation of the current findings.

A third possibility to consider is the joint occurrence of both functions in the rhizosphere, regardless of the taxa harboring them, thereby providing functional redundancy (Shade and Handelsman, 2012). Several studies in soil or aquatic settings have suggested that the metabolic/functional potential of microbial communities rather than their taxonomic variations are closely related to environmental conditions (Bouffaud et al. 2018; Burke et al. 2011; Louca et al. 2016; Louca et al. 2017). These observations were conceptualized as the "It's the song, not the singer" theory (ITSNTS; Doolittle and Booth 2017), i.e. functional groups within microbial communities (the songs) would be better conserved and more relevant ecologically than the taxa themselves (the singers). Consistent with the ITSNTS theory, our study suggests that the assembly of the rhizosphere microbial community would entail a balance between phytostimulation-relevant genes, which may be needed to achieve an effective holobiont (i.e., the plant host and its functional microbiota), and points to the preponderance of functional interactions within the plant holobiont. This hypothesis, which has been put forward recently for root-associated microorganisms (Lemanceau et al. 2017), remains speculative at this stage and deserves further research attention. In particular, methodology development is needed to enable direct assessment of key plant-beneficial groups when parallel monitoring of several genes is required (e.g. for auxin production or P solubilization, which entail many genetic pathways), in contrast to ACC deamination and N fixation for which analysis of a single gene (*acdS* and *nifH*, respectively) may suffice.

To test whether the current findings could be also relevant under other environmental conditions, we reassessed the data obtained for *nifH* (Bouffaud et al. 2016) and *acdS* (Bouffaud

et al. 2018) from two maize lines grown in another soil (luvisol) with different management histories (cropped soil vs meadow soil). A positive correlation (r = 0.45 ; P = 0.050 ; n = 20) was found between the numbers of *nifH* and *acdS* bacteria in the monocropping soil but not in meadow soil (P = 0.75 ; n = 10), suggesting that maize monocropping history could have been an important factor. However, these findings were obtained with young plants only (21 days), grown in sieved soil under greenhouse conditions.

In conclusion, the current findings indicate that rhizobacteria with nitrogen fixation capacity and counterparts harboring ACC deamination ability co-occur in the maize rhizosphere, pointing to the possibility that plants may rely on multiple, complementary phytostimulatory functions provided by their microbial partners. Additional method development is needed to extend this type of assessment to additional phytostimulatory groups and other microbial functional groups important for plant performance.

ACKNOWLEDGEMENTS

This work was supported in part by project Azodure (ANR Agrobiosphère ANR-12-AGRO-0008). We are grateful to J. Haurat and H. Brunet for technical help, as well as D. Abrouk (iBio platform, UMR CNRS 5557 Écologie Microbienne) and J. Thioulouse (UMR CNRS LBBE) for helpful discussion. The authors declare no conflict of interest.

DATA ACCESSIBILITY

Illumina MiSeq paired-end reads have been deposited in the European Bioinformatics Institute (EBI) database under accession numbers PRJEB14347 (ERP015984) for *rrs*; PRJEB14346 (ERP015983) for *nifH*, PRJEB14343 (ERP015981) for *acdS*.

AUTHOR CONTRIBUTIONS

LL, YML and DM designed the project, SR, LL, CPC, YML and DM carried out field work and samplings, SR conducted the molecular work, SR, MLB and AD implemented bioinformatic analyses, SR, YML and DM analyzed data, SR, YML and DM prepared the first draft of the manuscript, which was finalized by all authors.

REFERENCES

Achouak W, Normand P, Heulin T. Comparative phylogeny of *rrs* and *nifH* genes in the *Bacillaceae*. *Int J Syst Evol Microbiol* 1999;*49*(3):961-967. doi:10.1099/00207713-49-3-961

Agaras BC, Scandiani M, Luque A *et al.* Quantification of the potential biocontrol and direct plant growth promotion abilities based on multiple biological traits distinguish different groups of *Pseudomonas* spp. isolates. *Biological Control* 2015;*90*:173-186. doi:https://doi.org/10.1016/j.biocontrol.2015.07.003

Almario J, Gobbin D, Défago G *et al.* Prevalence of type III secretion system in effective biocontrol pseudomonads. *Res Microbiol* 2014;*165*(4):300-304. doi:https://doi.org/10.1016/j.resmic.2014.03.008

Almario J, Muller D, Défago G *et al.* Rhizosphere ecology and phytoprotection in soils naturally suppressive to Thielaviopsis black root rot of tobacco. *Environ Microbiol* 2014;*16*(7):1949-1960. doi:10.1111/1462-2920.12459

Arruda L, Beneduzi A, Martins A *et al.* Screening of rhizobacteria isolated from maize (*Zea mays* L.) in Rio Grande do Sul State (South Brazil) and analysis of their potential to improve plant growth. *Appl Soil Ecol* 2013;*63*:15-22. doi:https://doi.org/10.1016/j.apsoil.2012.09.001

Bakker MG, Schlatter DC, Otto-Hanson L *et al.* Diffuse symbioses: roles of plant–plant, plant–microbe and microbe–microbe interactions in structuring the soil microbiome. *Mol Ecol* 2014;*23*(6):1571-1583. doi:10.1111/mec.12571

Barberán A, Bates ST, Casamayor EO *et al.* Using network analysis to explore co-occurrence patterns in soil microbial communities. *ISME J* 2011;*6*:343–351. doi:10.1038/ismej.2011.119 https://www.nature.com/articles/ismej2011119#supplementary-information

Bashan Y, de-Bashan LE. Chapter Two - How the plant growth-promoting bacterium *Azospirillum* promotes plant growth—A critical assessment. In: Sparks DL (ed). *Advances in Agronomy*. Academic Press, 2010, 108, 77-136.

Bashan Y, de-Bashan LE, Prabhu SR *et al.* Advances in plant growth-promoting bacterial inoculant technology: formulations and practical perspectives (1998–2013). *Plant Soil* 2014;*378*(1):1-33. doi:10.1007/s11104-013-1956-x

Berg G, Smalla K. Plant species and soil type cooperatively shape the structure and function of microbial communities in the rhizosphere. *FEMS Microbiol Ecol* 2009;*68*(1):1-13. doi:10.1111/j.1574-6941.2009.00654.x

Bertalan M, Albano R, de Pádua V *et al.* Complete genome sequence of the sugarcane nitrogen-fixing endophyte *Gluconacetobacter diazotrophicus* Pal5. *BMC Genomics* 2009;*10*(1):450. doi:10.1186/1471-2164-10-450

Blaha D, Prigent-Combaret C, Mirza MS *et al.* Phylogeny of the 1-aminocyclopropane-1-carboxylic acid deaminase-encoding gene *acdS* in phytobeneficial and pathogenic Proteobacteria and relation with strain biogeography. *FEMS Microbiol Ecol* 2006;*56*(3):455-470. doi:10.1111/j.1574-6941.2006.00082.x

Bouffaud M-L, Renoud S, Dubost A *et al.* 1-Aminocyclopropane-1-carboxylate deaminase producers associated to maize and other Poaceae species. *Microbiome* 2018;*6*(1):114. doi:10.1186/s40168-018-0503-7

Bouffaud M-L, Renoud S, Moënne-Loccoz Y *et al.* Is plant evolutionary history impacting recruitment of diazotrophs and *nifH* expression in the rhizosphere? *Sci Rep* 2016;*6*:21690. doi:10.1038/srep21690 http://www.nature.com/articles/srep21690#supplementary-information

Boyd E, Peters J. New insights into the evolutionary history of biological nitrogen fixation. *Front Microbiol* 2013;*4*:201. doi:10.3389/fmicb.2013.00201

Bruto M, Prigent-Combaret C, Luis P *et al.* Frequent, independent transfers of a catabolic gene from bacteria to contrasted filamentous eukaryotes. *Proc R Soc Lond B: Biol Sci* 2014;*281*:1789. doi:10.1098/rspb.2014.0848

Bruto M, Prigent-Combaret C, Muller D *et al.* Analysis of genes contributing to plant-beneficial functions in plant growth-promoting rhizobacteria and related Proteobacteria. *Sci Rep* 2014;*4*:6261. doi:10.1038/srep06261

519 Burke C, Steinberg P, Rusch D *et al.* Bacterial community assembly based on functional genes rather
520 than species. *Proc Natl Acad Sci USA* 2011;*108*(34):14288-14293.
521 doi:10.1073/pnas.1101591108

522 Cassán F, Vanderleyden J, Spaepen S. Physiological and agronomical aspects of phytohormone
523 production by model Plant-Growth-Promoting Rhizobacteria (PGPR) belonging to the genus
524 *Azospirillum*. *J. Plant Growth Regul* 2014;*33*(2):440-459. doi:10.1007/s00344-013-9362-4

525 Chen XH, Koumoutsi A, Scholz R *et al.* Comparative analysis of the complete genome sequence of
526 the plant growth–promoting bacterium *Bacillus amyloliquefaciens* FZB42. *Nature Biotechnol*
527 2007;*25*:1007. doi:10.1038/nbt1325 https://www.nature.com/articles/nbt1325#supplementary-
528 information

529 Chessel D, Dufour AB, Thioulouse J. The ade4 package-I-One-table methods. *R News* 2004;*4*(1):5-10.

530 Cormier F, Foulkes J, Hirel B *et al.* Breeding for increased nitrogen-use efficiency: a review for wheat
531 (*T. aestivum* L.). *Plant Breeding* 2016;*135*(3):255-278. doi:10.1111/pbr.12371

532 Couillerot O, Ramírez-Trujillo A, Walker V *et al.* Comparison of prominent *Azospirillum* strains in
533 *Azospirillum–Pseudomonas–Glomus* consortia for promotion of maize growth. *Appl*
534 *Microbiol Biotechnol* 2013;*97*(10):4639-4649. doi:10.1007/s00253-012-4249-z

535 Culhane AC, Thioulouse J, Perrière G *et al.* MADE4: an R package for multivariate analysis of gene
536 expression data. *Bioinformatics* 2005;*21*(11):2789-2790. doi:10.1093/bioinformatics/bti394

537 Deynze A, Zamora P, Delaux P-M *et al.* Nitrogen fixation in a landrace of maize is supported by a
538 mucilage-associated diazotrophic microbiota. *PLoS Biol* 2018;*16*(8):e2006352. https://doi-
539 org.inee.bib.cnrs.fr/10.1371/journal.pbio.2006352

540 DeSantis TZ, Hugenholtz P, Larsen N *et al.* Greengenes, a chimera-checked 16S rRNA gene database
541 and workbench compatible with ARB. *Appl Environ Microbiol* 2006;*72*(7):5069-5072.
542 doi:10.1128/aem.03006-05

543 Doolittle WF, Booth A. It's the song, not the singer: an exploration of holobiosis and evolutionary
544 theory. *Biol Philos* 2017;*32*(1):5-24. doi:10.1007/s10539-016-9542-2

Dray S, Chessel D, Thioulouse J. Co-inertia analysis and the linking of ecological data tables. *Ecology* 2003;*84*(11):3078-3089. doi:10.1890/03-0178

Dray S, Dufour AB, Chessel D. The ade4 Package—II: Two-table and K-table methods. *R News* 2007;*7*:47-52.

Duan J, Müller KM, Charles T *et al.* 1-aminocyclopropane-1-carboxylate (ACC) deaminase genes in Rhizobia from southern Saskatchewan. *Microb Ecol* 2009;*57*(3):423-436. doi:10.1007/s00248-008-9407-6

Frapolli M, Pothier JF, Défago G *et al.* Evolutionary history of synthesis pathway genes for phloroglucinol and cyanide antimicrobials in plant-associated fluorescent pseudomonads. *Mol Phylogenet Evol* 2012;*63*(3):877-890. doi:https://doi.org/10.1016/j.ympev.2012.02.030

Freilich S, Kreimer A, Meilijson I *et al.* The large-scale organization of the bacterial network of ecological co-occurrence interactions. *Nucleic Acids Res* 2010;*38*(12):3857-3868. doi:10.1093/nar/gkq118

Gaby JC, Buckley DH. The use of degenerate primers in qPCR analysis of functional genes can cause dramatic quantification bias as revealed by investigation of *nifH* primer performance. *Microb Ecol* 2017;*74*(3):701-708. doi:10.1007/s00248-017-0968-0

Gamalero E, Glick BR. Bacterial modulation of plant ethylene levels. *Plant Physiol* 2015;*169*(1):13-22. doi:10.1104/pp.15.00284

Glick BR. Bacteria with ACC deaminase can promote plant growth and help to feed the world. *Microbiol Res* 2014;*169*(1):30-39. doi:https://doi.org/10.1016/j.micres.2013.09.009

Hartman K, van der Heijden MGA, Wittwe RA *et al.* Cropping practices manipulate abundance patterns of root and soil microbiome members paving the way to smart farming. *Microbiome* 2018;*6*(1):14. doi:10.1186/s40168-017-0389-9

Jha B, Gontia I, Hartmann A. The roots of the halophyte *Salicornia brachiata* are a source of new halotolerant diazotrophic bacteria with plant growth-promoting potential. *Plant Soil* 2012;*356*(1):265-277. doi:10.1007/s11104-011-0877-9

Lassalle F, Muller D, Nesme X. Ecological speciation in bacteria: reverse ecology approaches reveal the adaptive part of bacterial cladogenesis. *Res Microbiol* 2015;*166*(10):729-741. doi:https://doi.org/10.1016/j.resmic.2015.06.008

Lemanceau P, Blouin M, Muller D, *et al.* Let the core microbiota be functional. *Trends Plant Sci* 2017;*22*(7):583-595. doi:https://doi.org/10.1016/j.tplants.2017.04.008

Li Z, Chang S, Ye S *et al.* Differentiation of 1-aminocyclopropane-1-carboxylate (ACC) deaminase from its homologs is the key for identifying bacteria containing ACC deaminase. *FEMS Microbiol Ecol* 2015;*91*(10):fiv112-fiv112. doi:10.1093/femsec/fiv112

Louca S, Parfrey LW, Doebeli M. Decoupling function and taxonomy in the global ocean microbiome. *Science* 2016;*353*(6305):1272-1277. doi:10.1126/science.aaf4507

Louca S, Jacques SMS, Pires APF *et al.* High taxonomic variability despite stable functional structure across microbial communities. *Nat Ecol Evol* 2017;*1*:0015. doi:10.1038/s41559-016-0015

Ma W, Guinel FC, Glick, BR. *Rhizobium leguminosarum* biovar *viciae* 1-aminocyclopropane-1-carboxylate deaminase promotes nodulation of pea plants. *Appl Environ Microbiol* 2003;*69*(8):4396-4402. doi:10.1128/aem.69.8.4396-4402.2003

Mårtensson L, Díez B, Wartiainen I *et al.* Diazotrophic diversity, *nifH* gene expression and nitrogenase activity in a rice paddy field in Fujian, China. *Plant Soil* 2009;*325*(1):207-218. doi:10.1007/s11104-009-9970-8

Nascimento FX, Brígido C, Glick BR *et al.* ACC deaminase genes are conserved among *Mesorhizobium* species able to nodulate the same host plant. *FEMS Microbiol Lett* 2012;*336*(1):26-37. doi:10.1111/j.1574-6968.2012.02648.x

Nukui N, Minamisawa K, Ayabe S-I *et al.* Expression of the 1-aminocyclopropane-1-carboxylic acid deaminase gene requires symbiotic nitrogen-fixing regulator gene *nifA2* in *Mesorhizobium loti* MAFF303099. *Appl Environ Microbiol* 2006;*72*(7):4964-4969. doi:10.1128/aem.02745-05

Pieterse CMJ, Van Wees SCM. Induced disease resistance. In: Lugtenberg B (ed). *Principles of Plant-Microbe Interactions: Microbes for Sustainable Agriculture*. Springer International Publishing, 2015, 123-33.

Pii Y, Mimmo T, Tomasi N *et al.* Microbial interactions in the rhizosphere: beneficial influences of plant growth-promoting rhizobacteria on nutrient acquisition process. A review. *Biol Fertil Soils* 2015;*51*(4):403-415. doi:10.1007/s00374-015-0996-1

Poly F, Jocteur Monrozier L, Bally R. Improvement in the RFLP procedure for studying the diversity of *nifH* genes in communities of nitrogen fixers in soil. *Res Microbiol* 2001;*152*(1):95-103. doi:https://doi.org/10.1016/S0923-2508(00)01172-4

Prigent-Combaret C, Blaha D, Pothier J *et al.* Physical organization and phylogenetic analysis of *acdR* as leucine-responsive regulator of the 1-aminocyclopropane-1-carboxylate deaminase gene *acdS* in phytobeneficial *Azospirillum lipoferum* 4B and other *Proteobacteria*. *FEMS Microbiol Ecol* 2008;*65*(2):202-219. doi:10.1111/j.1574-6941.2008.00474.x

Puri A, Padda KP, Chanway CP. Evidence of nitrogen fixation and growth promotion in canola (*Brassica napus* L.) by an endophytic diazotroph *Paenibacillus polymyxa* P2b-2R. *Biol Fertil Soils* 2016;*52*(1):119-125. doi:10.1007/s00374-015-1051-y

Raaijmakers JM, Paulitz TC, Steinberg C *et al.* The rhizosphere: a playground and battlefield for soilborne pathogens and beneficial microorganisms. *Plant Soil* 2009;*321*(1):341-361. doi:10.1007/s11104-008-9568-6

Rana A, Saharan B, Joshi M *et al*. Identification of multi-trait PGPR isolates and evaluating their potential as inoculants for wheat. *Ann Microbiol* 2011;*61*(4):893-900. doi:10.1007/s13213-011-0211-z

Redondo-Nieto M, Barret M, Morrissey J *et al.* Genome sequence reveals that *Pseudomonas fluorescens* F113 possesses a large and diverse array of systems for rhizosphere function and host interaction. *BMC Genomics* 2013;*14*(1):54. doi:10.1186/1471-2164-14-54

Rozier C, Hamzaoui J, Lemoine D *et al.* Field-based assessment of the mechanism of maize yield enhancement by *Azospirillum lipoferum* CRT1. *Sci Rep* 2017;*7*(1):7416. doi:10.1038/s41598-017-07929-8

Shade A, Handelsman J. Beyond the Venn diagram: the hunt for a core microbiome. *Environ Microbiol* 2012;*14*(1):4-12. doi:10.1111/j.1462-2920.2011.02585.x

Team, R. *R: A Language and Environment for Statistical Computing* 2014. Vienna, Austria: R Foundation for Statistical Computing.

Vacheron J, Desbrosses G, Bouffaud M-L *et al.* Plant growth-promoting rhizobacteria and root system functioning. *Front Plant Sci* 2013;*4*:356. doi:10.3389/fpls.2013.00356

Vacheron J, Desbrosses G, Renoud S *et al.* Differential contribution of plant-beneficial functions from *Pseudomonas kilonensis* F113 to root system architecture alterations in *Arabidopsis thaliana* and *Zea mays*. *Mol Plant-Microbe Interact* 2017;*31*(2):212-223. doi:10.1094/MPMI-07-17-0185-R

Vacheron J, Moënne-Loccoz Y, Dubost A *et al.* Fluorescent *Pseudomonas* strains with only few plant-beneficial properties are favored in the maize rhizosphere. *Front Plant Sci* 2016;*7*:1212. doi:10.3389/fpls.2016.01212

Vandenkoornhuyse P, Quaiser A, Duhamel *et al.* The importance of the microbiome of the plant holobiont. *New Phytol* 2015;*206*(4):1196-1206. doi:doi:10.1111/nph.13312

Vinuesa P, Silva C, Lorite MJ *et al.* Molecular systematics of rhizobia based on maximum likelihood and Bayesian phylogenies inferred from *rrs*, *atpD*, *recA* and *nifH* sequences, and their use in the classification of *Sesbania* microsymbionts from Venezuelan wetlands. *Syst Appl Microbiol* 2005;*28*(8):702-716. doi:https://doi.org/10.1016/j.syapm.2005.05.007

Wang Y, Zhu G, Harhangi HR *et al.* Co-occurrence and distribution of nitrite-dependent anaerobic ammonium and methane-oxidizing bacteria in a paddy soil. *FEMS Microbiol Lett* 2012;*336*(2):79-88. doi:10.1111/j.1574-6968.2012.02654.x

Wartiainen I, Eriksson T, Zheng W *et al.* Variation in the active diazotrophic community in rice paddy—*nifH* PCR-DGGE analysis of rhizosphere and bulk soil. *Appl Soil Ecol* 2008;*39*(1):65-75. doi:https://doi.org/10.1016/j.apsoil.2007.11.008

Wisniewski-Dyé F, Lozano L, Acosta-Cruz E *et al.* Genome sequence of *Azospirillum brasilense* CBG497 and comparative analyses of *Azospirillum* core and accessory genomes provide insight into niche adaptation. *Genes* 2012;*3*(4):576.

Zehr JP, Jenkins BD, Short SM *et al.* Nitrogenase gene diversity and microbial community structure: a cross-system comparison. *Envirol Microbiol* 2003;*5*(7):539-554. doi:10.1046/j.1462-2920.2003.00451.x

Zehr JP, McReynolds LA. Use of degenerate oligonucleotides for amplification of the *nifH* gene from the marine cyanobacterium *Trichodesmium thiebautii*. *Appl Environ Microbiol* 1989;*55*(10):2522-2526.

Legend

FIGURE 1. Size of the *acdS* and *nifH* functional groups compared in the three field sites L, FC and C over four sampling times. Means and standard deviations are shown for the *acdS* group at 6 leaves in 2014 (A) and 2015 (B) and at flowering in 2014 (E) and 2015 (F) and for the *nifH* group at 6 leaves in 2014 (C) and 2015 (D) and at flowering in 2014 (G) and 2015 (H). The analysis was done using pooled samples of six roots systems (n= 5) at FC and C and individual root systems (n = 30) at L in 2014, and individual root systems (n = 20) at all three sites in 2015. Statistical differences between sites are indicated by letters a-c (ANOVA and Fischer's LSD tests, $P < 0.05$).

FIGURE 2. Correlation between log numbers of *nifH* (X axis) and *acdS* genes (Y axis). Correlation was established using the Pearson coefficient. The analysis was done using pooled samples of six roots systems (n= 5) at FC and C and individual root systems (n = 30) at L in 2014, and individual root systems (n = 20) at all three sites in 2015.

FIGURE 3. Correlation between Shannon diversity indices of *nifH* and *acdS* (A), Simpson diversity indices of *nifH* and *acdS* (B), Shannon diversity indices of *rrs* and *acdS* or *nifH* (C), and Simpson diversity indices of *rrs* and *acdS* or *nifH* (D). Correlation was established separately at each of the three field sites L, FC and C, using the Pearson coefficient (n = 5).

FIGURE 4. Comparison of *nifH* (A), *acdS* (B) and *rrs* (C) diversity between sites L, FC and C by between-class analysis. Red circles, green triangles and blue squares are used for samples from sites FC, C and L, respectively. The curves at the top and the left of the panels show the distribution of samples on respectively the X and Y axes.

FIGURE 5. Co-inertia analysis between *acdS* and *nifH* diversities (A), *rrs* and *nifH* diversities (B) and *rrs* and *acdS* diversities (C). Projection of the samples (n = 5) is based on both *acdS* (Blue) and *nifH* (Green), *rrs* (Grey) and *nifH* (Green), or *rrs* (Grey) and *acdS* (Blue) diversity variables (level = genus) into a same factorial plan. The vector in black shows the strength of co-trends between the two barycenters of variables as related to each site (L, FC, C). Shorter vectors indicate stronger convergent trends between the two variable groups.

FIGURE S1: Rarefaction curves for *nifH* (A), *acdS* (B) and *rrs* (C) genes**.**

FIGURE S2. RAxML bipartition tree of 3322 sequenced *acdS* alleles from *Poaceae* rhizosphere. The tree was visualized using iTOL software (Letunic I, Bork P. Interactive Tree Of Life (iTOL) v4: recent updates and new developments (2019) *Nucleic Acids Res* doi: 10.1093/nar/gkz239). Branches colored in violet represent the out-group of D-cystein desulfhydrase genes, whereas *acdS* alleles affiliated to *Betaproteobacteria* are shown in khaki, to *Gammaproteobacteria* in blue, to *Actinobacteria* in green, to *Alphaproteobacteria* in red, and to microeukaryotes in orange. The tree can be viewed online at the following link http://itol.embl.de/shared/*acdStree*.

Table 1. Field characteristics of the top (5-30 cm) soil layer.

Field	Soil type	Texture (%)			pH		Organic C	Total N	C/N ratio	Cation exchange (cmol/kg)			
		Sand	Silt	Clay	H_2O	KCl	(g/kg)	(g/kg)		CEC[a]	Ca^{2+}	Mg^{2+}	K^+
FC	Fluvic cambisol	26.9	38.3	34.7	7.1	6.3	31.6	3.4	9.3	22.8	21.2	0.67	0.38
L	Luvisol	42.9	42.9	14.2	7.3	6.7	21.5	1.6	13.4	93.0	10.5	0.33	0.43
C	Calcisol	15.6	74.1	10.3	8.2	7.7	25.9	3.1	8.4	97.0	36.1	0.24	0.29

[a]CEC, cation exchange capacity.

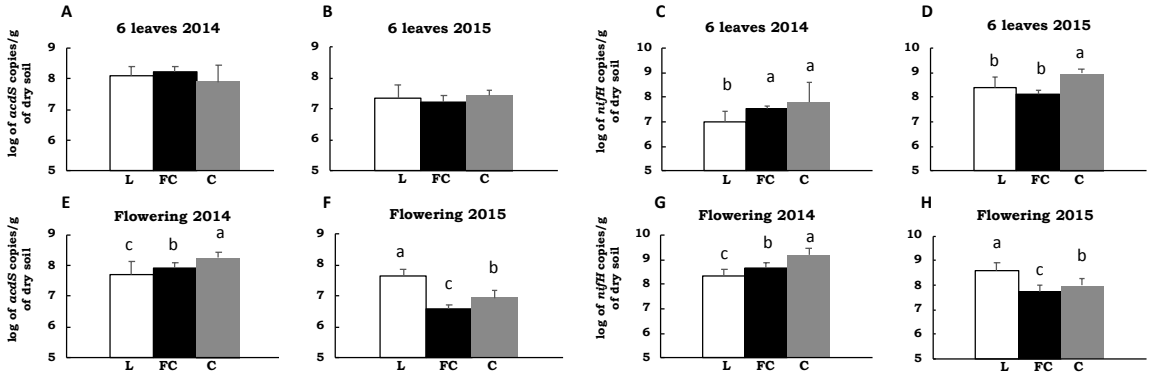

Fig. 1

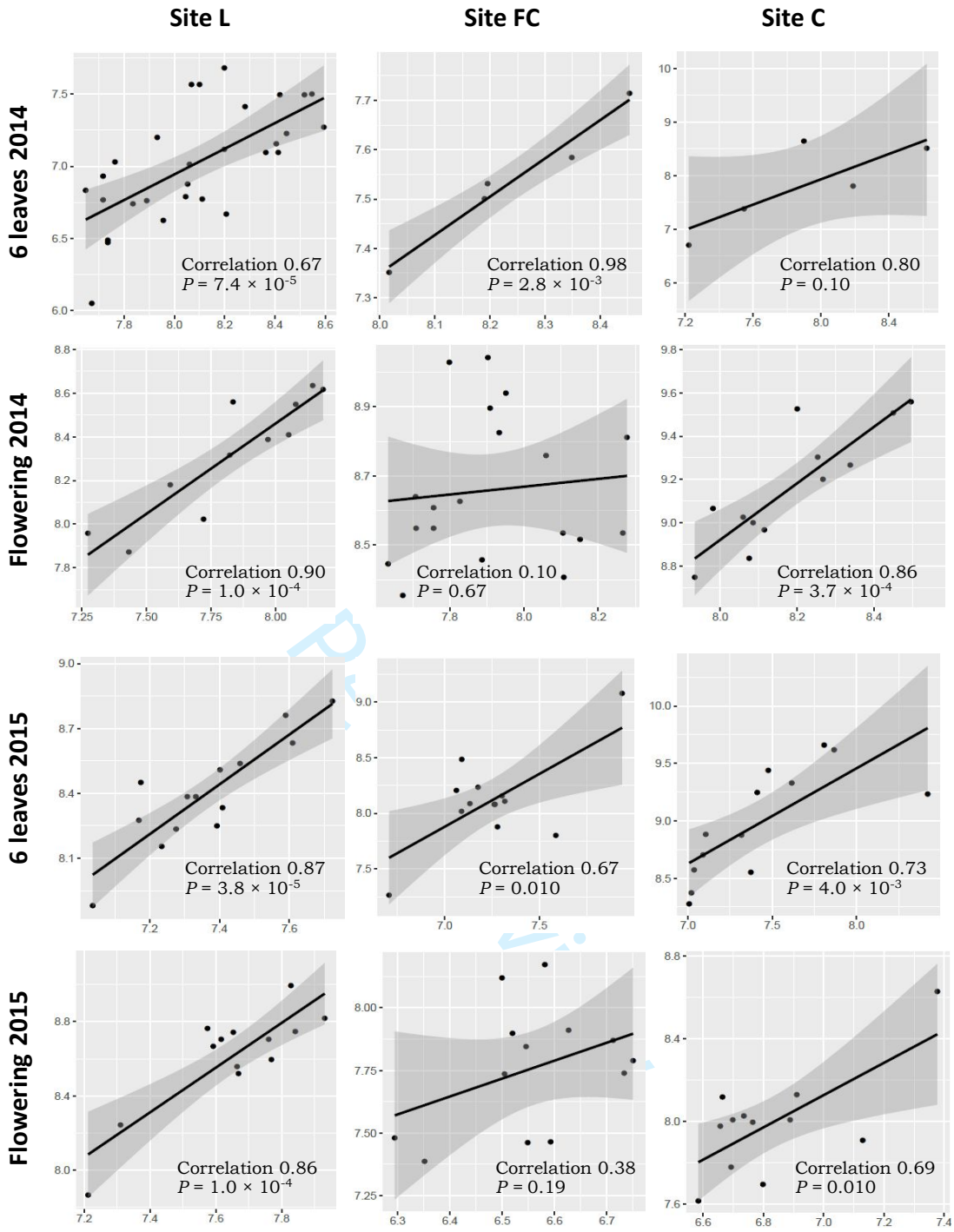
Site L
Site FC
Site C
6 leaves 2014
Flowering 2014
6 leaves 2015
Flowering 2015
Correlation 0.67
P = 7.4 × 10-5
Correlation 0.98
P = 2.8 × 10-3
Correlation 0.80
P = 0.10
Correlation 0.90
P = 1.0 × 10-4
Correlation 0.10
P = 0.67
Correlation 0.86
P = 3.7 × 10-4
Correlation 0.87
P = 3.8 × 10-5
Correlation 0.67
P = 0.010
Correlation 0.73
P = 4.0 × 10-3
Correlation 0.86
P = 1.0 × 10-4
Correlation 0.38
P = 0.19
Correlation 0.69
P = 0.010

Fig. 2

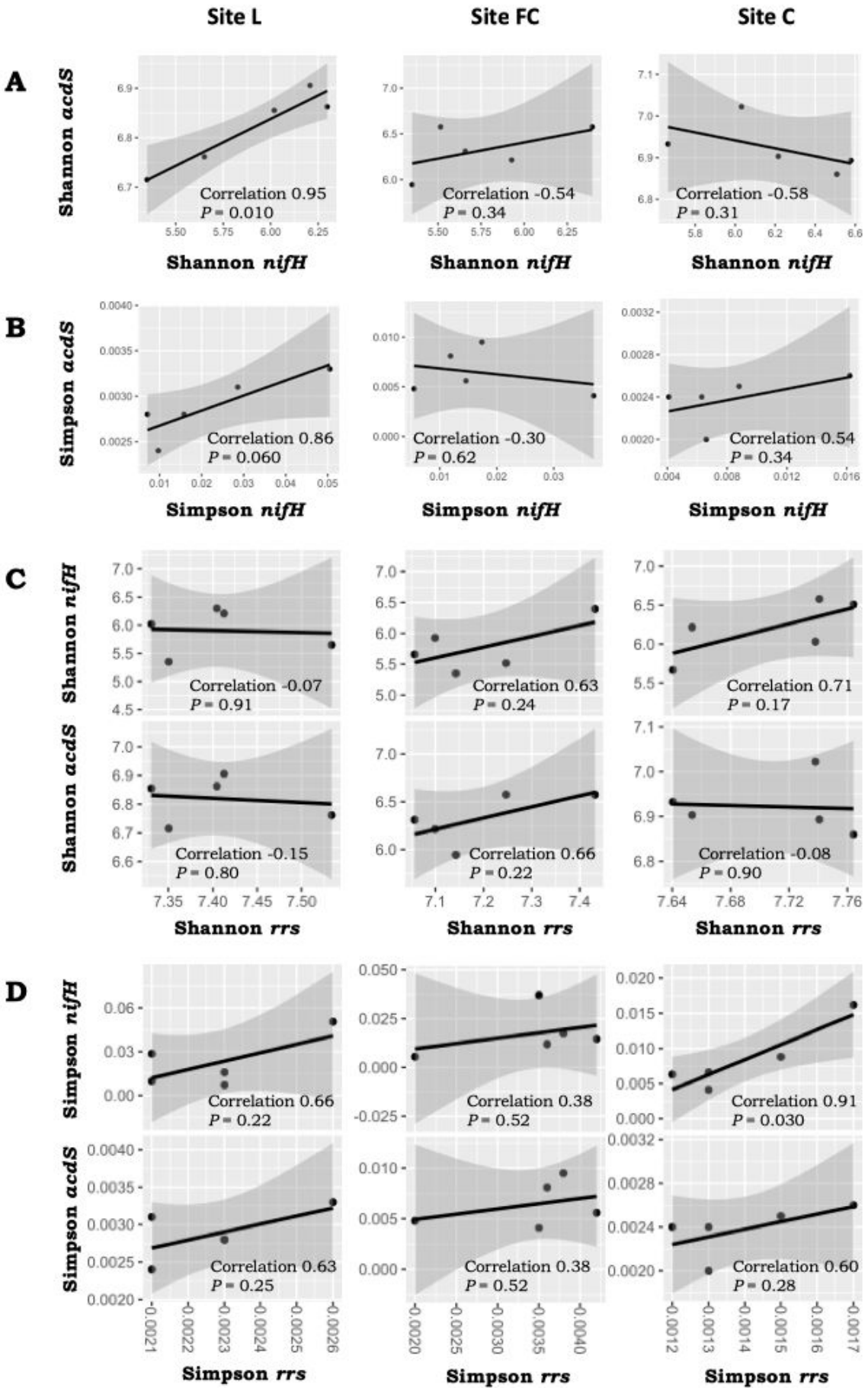

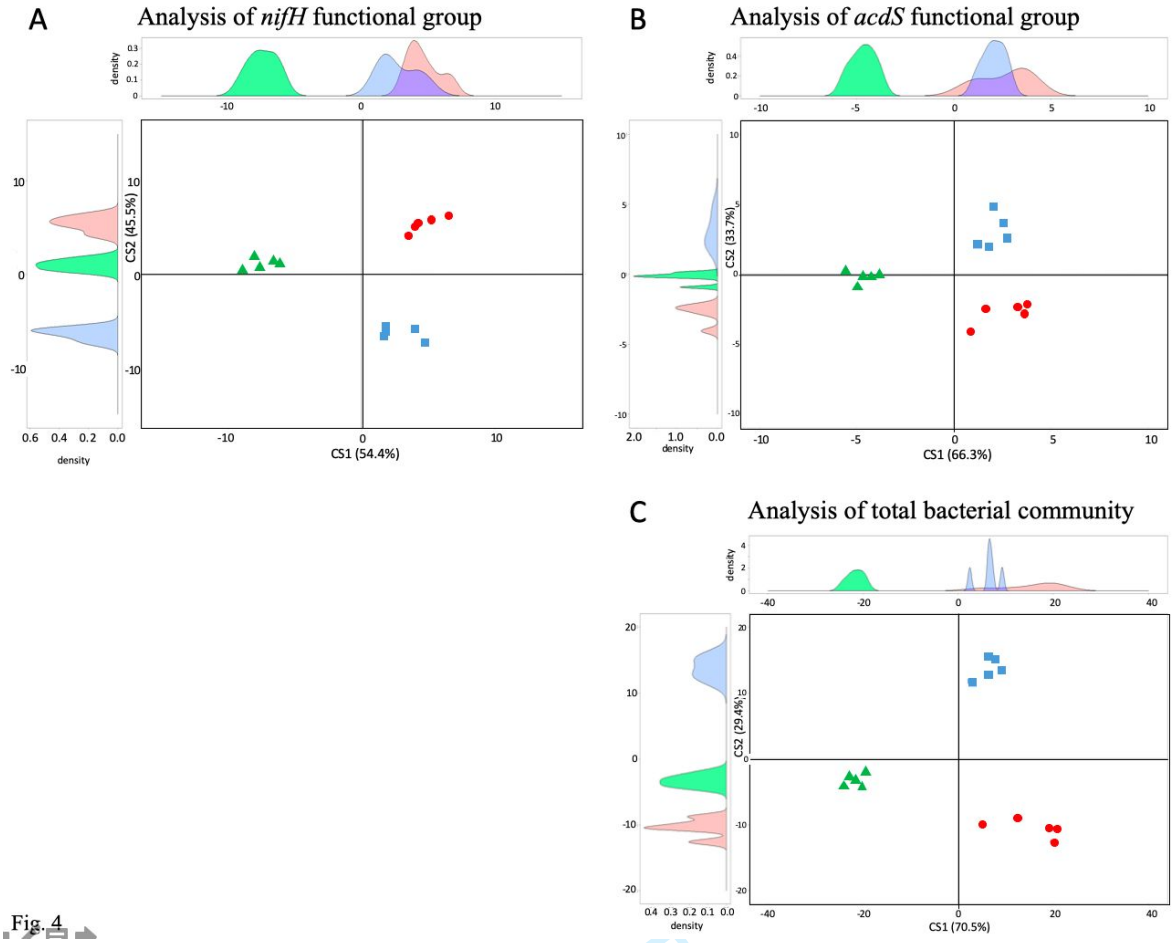

Fig. 4

Figure 5